THESIS FOR THE DEGREE OF DOCTOR OF PHILOSOPHY

Exploring the role of rheology in bolus flow using an *in vitro* approach

Waqas Muhammad

Department of Industrial and Materials Science

CHALMERS UNIVERSITY OF TECHNOLOGY

SE-412 96 Gothenburg

Sweden

Exploring the role of rheology in bolus flow using an in vitro approach

The experimental work was performed at the RISE Agrifood and Bioscience, Department of Product Design and Perception

ISBN: 978-91-7597-847-5

Serial number: 4528

Ny serie: ISSN0346-718X

Department of Industrial and Materials Science

Chalmers University of Technology

SE-412 96 Gothenburg

Sweden

Printed by: Chalmers digitaltryck

Gothenburg, Sweden

Cover image: Model pharynx cavity showing the bolus flow died blue (left image), bolus flow in actual human swallowing during one of our clinical studies (middle image) and the velocity profile acquired in the *in vitro* model developed in this work (right image)

Exploring the role of rheology in bolus flow using an *in vitro* approach

WAQAS MUHAMMAD

Research Institutes of Sweden and

Chalmers University of Technology

Gothenburg, Sweden

ABSTRACT

Swallowing disorders, termed 'dysphagia', are more common in the elderly but can also affect younger persons. Approximately, 8% of the world's population suffers from dysphagia. A Texture Modified Diet (TMD), which increases bolus viscosity to adjust for the sluggish bolus handling mechanism, is the most common intervention. Other rheological properties, such as bolus elasticity, shear rate, and yield stress, are often ignored. TMDs, which often comprise gum- and starch-based thickeners, were characterised for their rheological properties. The gum-based thickeners were considerably more elastic and exhibited a mild yield stress, showing a fine-stranded network structure on the nanoscale length when visualised by electron microscopy, as compared to the starch-based thickeners. Among the rheological properties, elasticity is cited as the most important for safe swallowing. Therefore, an *in vivo* study was performed in which fluids that have elastic properties were assessed for efficacy of safe swallowing in patients with dysphagia. These fluids showed easy swallowability, in terms of the sensory response and transit times during the oral and pharyngeal stages. While clinical examination is the standard and most appropriate way to diagnose dysphagia, difficulties arise in relation to the use of contrast media, ethics, and patient discomfort. To overcome these difficulties and to reduce the frequency of clinical analysis, an *in vitro* approach was adopted. And an *in vitro* swallowing model was developed that can be used to perform experimental bolus visualisation and manometry, mimicking the *in vivo* counterpart of video fluoroscopy and manometry. To study bolus transport, Pulsed Ultrasound Doppler Velocimetry was used. Pressure sensors were embedded in the model pharynx body to measure the bolus pressure during transit. The device delivers the bolus, at an appropriate speed and volume, and can handle boluses with different consistencies. In the device, bolus velocities ranging from 0.04 m/s to 0.48 m/s were measured, while bolus consistency was varied from nectar-thick to pudding-thick following National Dysphagia Diet scale. These velocities are within the range that is often reported for *in vivo* experiments. The acquired velocities yielded shear rates in the range of 13–229 s^{-1}, which is both lower and mostly higher shear rates than 50s^{-1} commonly referred to for deglutition. Similarly, when gum and starch-thickened boluses were injected into the model pharynx, the starch-thickened bolus often disintegrated, leaving residues in the model pharynx. When thickened boluses were analysed using manometry, by varying the bolus composition, shape, and volume, the pressure values at different locations in the model pharynx were in the range often noticed in clinical assessments. The device can simulate abnormal swallowing conditions, such as delayed epiglottis and Upper Esophageal Sphincter (UES) closure. Simulations of abnormal UES conditions, i.e. reduced UES area, yielded different pressure values in the lower pharynx. Therefore, the device can be used as a pre-clinical study tool to elucidate the relationship between bolus rheology and deglutition.

Keywords: Bolus rheology, dysphagia, *in vitro* simulations, *in vivo* analysis, ultrasound viscometry, extensional rheology, *in vitro* manometry, microstructure analysis, thickened fluids

List of papers

The thesis is based on the following four papers

1. **Effects of rheological factors on perceived ease of swallowing**

   M. Nyström, Waqas M Qazi, M. Bülow, O. Ekberg and M. Stading.

   Journal of applied rheology. 2015. Volume 25, 6

2. **Shear and extensional rheology of commercial thickeners used for dysphagia management**

   Waqas M Qazi, J. Wiklund, A. Altskär O. Ekberg and M. Stading.

   Journal of texture studies. 2017. Volume 48, issue 6, p. 507-517

3. **A device that models human swallowing**

   M. Stading; Waqas M Qazi; F. Holmberg; J. Wiklund; R. Kotze O. Ekberg

   In press (Journal of dysphagia)

4. **Assessment of the food-swallowing process using bolus visualisation and manometry simultaneously in a device that models human swallowing**

   Waqas M Qazi, Olle Ekberg , Johan Wiklund, Reinhardt Kotze and Mats Stading

   In press (Journal of dysphagia)

Publication not included in the thesis

Simulation of *in vitro* swallowing

Waqas M Qazi and Stading M. (2017) *In vitro* Models for Simulating Swallowing. In: Ekberg O. (eds) Dysphagia. Medical Radiology. Springer, Cham.**DOI** https://doi.org/10.1007/174_2017_116

Contribution in papers

1. The author was responsible for the clinical study, experimental work and contributed to the writing of the manuscript. The sensory study on healthy subjects was performed by sensory experts at RISE

2. The author was responsible for planning all the experimental work and writing of the manuscript. Microscopy experiments performed by the microscopy experts at RISE.

3. The author contributed to the planning of how the device should be constructed, performed all the experimental work and manuscript writing.

4. The author was responsible for planning of the research, execution of experimental work and manuscript writing.

List of abbreviations

CaBER	Capillary Break up Extensional Rheometer
D	Diameter
η_E	Extensional viscosity
η	Shear viscosity (Pa.s)
σ	Stress (Pa)
$\dot{\varepsilon}$	Extension rate (s^{-1})
$\dot{\gamma}$	Shear rate (s^{-1})
ε_H	Hencky strain
ΔP	Pressure difference
UVP+PD	Ultrasound Pulsed Velocimetry + Pressure Drop
T_y	Yield stress
$\dot{m}$	Mass flow rate
$\dot{Q}$	Volumetric flow rate
r_o	Inlet radius
r_1	Outlet radius
HCF	Hyperbolic Contraction Flow
LM	Light Microscopy
NDD	National Dysphagia Diet
OTT	Oral Transit time
PTT	Pharyngeal Transit Time
PAA	Polyacrylamide
TEM	Transmission Electron Microscopy

Contents

1. INTRODUCTION

Deglutition or swallowing, which is the final stage of oral processing, is aimed at ensuring smooth transport of the orally processed food towards the stomach for further digestion. Swallowing is an involuntary action that occurs about 1,000 times a day, both voluntarily when we eat or drink foodstuffs or involuntarily when we swallow our own saliva (Mowlavi *et al.*, 2016) . Swallowing is composed of four stages: oral preparatory; oral; pharyngeal; and esophageal stage. Of these four stage, the pharyngeal stage of swallowing is the most crucial, as the pharynx is partly shared by the airways and food-swallowing tract (McFarland *et al.*, 2016). Misdirection of the bolus at the pharyngeal stage results in the bolus entering the airways, causing aspiration and possibly, pneumonia. Swallowing disorders (dysphagia) are estimated to affect 8% of the world population (Steele, 2015). Dysphagia is a growing concern in the developed world due to its ageing population. According to estimates, in Europe about 17% of the population is aged >65 years. The population of Sweden is expected to comprise 20% senior citizens (>65 years) by 2020. Epidemiological studies suggest that dysphagia occurs in up to 22% of people aged >50 years, while 40% of individuals who are more than 65 years old and are registered at the health-care centres suffer from dysphagia (Ekberg *et al.*, 2002).

The Modified Textured Diet is used to manage and nourish individuals who are suffering from dysphagia. The most commonly used approach is to increase the bolus viscosity using a thickener (gum- or starch-based) that is often available in the powdered form. The underlying theory is that a viscous food bolus travels at a lower velocity, thereby providing more time for the oropharyngeal apparatus to handle the bolus flow (Moret-Tatay *et al.*, 2015; C. Steele *et al.*, 2015; Tashiro *et al.*, 2010). The physiological responses of individuals who are suffering from dysphagia with neurological conditions or due to age-related impairment are insufficient for facilitating the rapid flow of foods or liquids through the oropharynx. Therefore, thickeners are added to the fluids to slow the bolus flow. Both gum and starch-based thickeners primarily increase the bolus consistency, although the mechanisms of thickening are different. Starch-based thickeners swell upon hydration, while gum-based thickeners form a network that retains water and increases the fluid viscosity.

Thickened fluids shear thins during flow, i.e., the perception of thickness decreases with increasing speed of deformation (Popa Nita *et al.*, 2013). The prediction of consistency during bolus transport requires appropriate knowledge of the shear rate during swallowing. A shear rate of 50 s^{-1}, taken from oral processing, is currently assumed to be the dominant parameter in pharyngeal swallowing. However, pharyngeal swallowing is rapid and shear rates higher than 50 s^{-1} have been predicted in some simulation studies. This results in a bolus of much lower consistency than is expected or suggested to the patients. In contrast, a bolus with high viscosity requires the exertion of a greater tongue propulsion force to push the bolus through the pharynx. High-viscosity boluses pushed by the tongue have been shown to increase the risk of post-swallow residues (Clavé *et al.*, 2006; C. Steele *et al.*, 2015).

A thickened fluid is normally designated so as to assist the health-care professional in preparing boluses of appropriate consistency for patients with swallowing disorders. Various countries, such as Japan, Australia, Denmark, Sweden, Ireland, the UK and US, have developed food consistency scales to characterise the textural properties of the dysphagia diet. Among these scales, the most noteworthy is the one implemented in the US as the National Dysphagia Diet (NDD). The NDD guidelines refer to the given range of consistencies at a shear rate of 50 s^{-1}, with 25ºC used as the reference temperature. The scale classifies fluids according to the following four consistencies:

1) Thin: 1–50 cp (0.001–0.05 Pa.s)
2) Nectar-like: 51–350 cp (0.05–0.35 Pa.s)
3) Honey-like: 350–1750 cp (0.35–1.75 Pa.s)
4) Spoon-thick: >1750 cp (>1.75 Pa.s)

The tools that are most often used by clinicians to examine dysphagia are manometry and video fluoroscopy, both of which are invasive techniques. Manometry is based on the insertion of a probe into the patient's pharynx, which may obstruct the bolus flow (Morinière *et al.*, 2013) and cause discomfort. Similarly, while performing video fluoroscopy, the swallowing of fluids is monitored using x-ray imaging, whereby the entire swallowing process is recorded, enabling the examiner to follow the swallowing sequence frame by frame (Bülow, 2003). Video fluoroscopy necessitates the use of contrast media, which are radio-opaque and alter the bolus rheology (Ekberg *et al.*, 2010).

The European Society for Swallowing Disorders (ESSD) in its recently published white paper (Newman *et al.*, 2016) has suggested the taking into acccount of rheological parameters, such as shear rate, the properties of non-Newtonian fluids, yield stress, elasticity, and density, in addition to the well-recognised parameter of shear viscosity (Gallegos *et al.*, 2016; Newman *et al.*, 2016). As the testing of these parameters directly in humans is problematic due to the lack of highly skilled operators, patient discomfort, and ethical issues, alternative methods are needed.

2. AIM AND OBJECTIVES

The main aim of this project was to develop a device that allows the examination of non-invasive *in vitro* swallowing, so as to elucidate the linkages between rheology and dysphagia management. The developed device should be able to simulate thickened bolus formation, bolus flow, and bolus measurements, i.e., similar to the tests performed in clinical studies.

Additional objectives were to characterise and examine the possibilities for applying other rheological parameters, such as shear rate, elasticity, and yield stress in both model and thickened fluids, and to test the potential of elasticity with respect to safe swallowing in cases of dysphagia.

To achieve this aim and objectives, a comprehensive approach was applied that can be broadly divided into:

- ✓ Clinical examination of the malfunctioned swallowing process
- To elucidate the linkages between fluid elasticity and safe swallowing (**Paper I**).

- ✓ Characterisation of the model fluids (composed of elasticity-providing ingredients) and thickened fluids (composed of gum- and starch-based thickeners)
- Characterisation of model fluids using extensional rheology, including shear rheology, microstructure characterisation, and yield stress measurements (**Paper II**).

- ✓ *In vitro* device construction and validation
- The *in vitro* swallowing model was constructed by taking into account the human pharyngeal geometry, the nature of bolus injection, simulations of actual physiological processes such as the closing of the vocal chords, the UES, the epiglottis, the opening of the nasopharyngeal passage upon bolus exit, and visual observations of the bolus.
- Bolus velocimetry and consequent shear rate measurements were performed during swallowing, for which a stand-alone ultrasound sensor system was developed.
- Non-invasive *in vitro* manometry was carried out using pressure sensors embedded into the model pharynx walls (**Paper III**).

- ✓ Application
- The developed device was used to simulate bolus flow in an *in vitro* analysis that mimics the *in vivo* counterpart. These analyses included manometry and bolus visualisation, using most of the consistencies mentioned in the NDD standards set by the American Dietetic Association (**Paper IV**).

3. BACKGROUND

3.1 Rheology

Rheology is the branch of science that deals with "the flow and deformation of matter". Rheology finds extensive applications in studies of polymers, foodstuffs, pharmaceuticals, and the interfacial interactions of materials. All types of shear behaviours, ranging from that of an ideal viscous liquid to the deformation of an ideal solid, can be described rheologically. When sheared under stress, an ideal viscous liquid, e.g., mineral oil, will deform irreversibly, i.e., all the mechanical energy supplied will be dissipated. An ideal solid material will store all the mechanical energy supplied, and it will recover completely and instantaneously once the stress is removed. However, all real-life materials exhibit both viscous and elastic behaviours, so they are viscoelastic (R. Paul Singh *et al.*, 2014).
Fluids can be deformed in shear and in extension. Shear rheology is a well-known for its beneficial effects phenomenon that is often used in the management of dysphagia, whereas extensional rheology, which is as important given that the bolus undergoes both shear and extensional deformations during swallowing, is often ignored. Extensional rheology is overlooked probably due to complications related to measuring material elongation properties.

3.1.1 Shear deformation

The concept of shear deformation can be explained by imagining a cube of fluid under flow (Fig. 1) that is deformed along its upper part. The given force, measured in Newtons (N), that deforms the material over a given area (m^2) is called the shear stress (σ), and it is expressed as F/A and measured in Pascals (N/m^2).

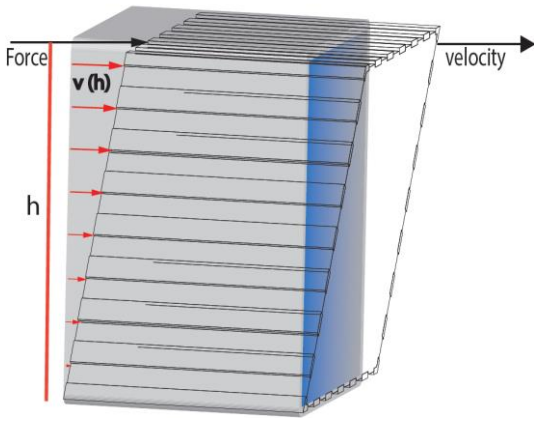

Figure 1: Cube fluid deformation upon application of a shear force.

The speed (v) with which this deformation takes place over a given height (h) is called the shear rate, which is expressed in 1/s ($\dot{\gamma} = v/h$) for an infinitely small cube. In other words, the shear rate is the derivative of the velocity profile, as described in Eq. [3.1]:

$$\dot{\gamma} = -\frac{dv(r)}{dr} \qquad [3.1]$$

The ratio of the two parameters of shear stress and shear rate provides the most familiar term in rheology: the shear viscosity $\eta = \sigma/\dot{\gamma}$ (expressed in Pa.s). Traditionally, shear rheology is measured using rotational rheometers. Various measurement geometries, such as cone-plate, plate-plate, and concentric cylinders, can be used depending on the type of sample being analysed.

In the research for this thesis, cone-plate or plate-plate geometry was mainly used to measure the shear viscosity owing to the samples being highly soluble and homogeneous in general. A schematic of these two geometries is given in Fig. 2.

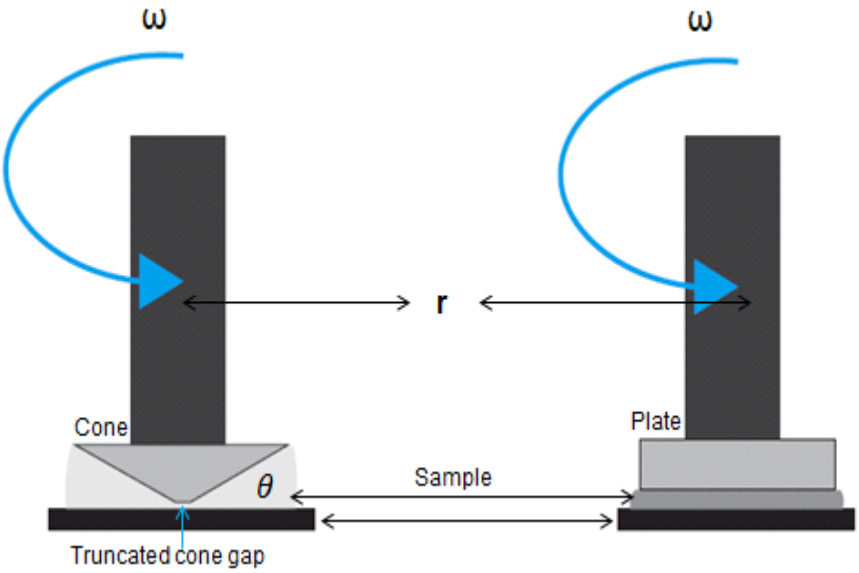

Figure 2: Cone plate (left) and plate-plate geometries used for shear rheology measurements.

Besides the traditional laboratory-based rheometry, Doppler Ultrasound Viscometry+Pressure Drop (UVP+PD), which can be considered as an advanced version of tube viscometry, was used in the in this work. Many biological fluid flows, such as blood flow in arteries and veins, air flow in pulmonary airways, and bolus flow during swallowing, occur in a tubular fashion. The application of Doppler ultrasound to measure blood flow is well-established in medical ultrasound examinations (Nahar *et al.*, 2012). Measurements of bolus/fluid flow during swallowing are not performed as commonly and, to the best of our knowledge, have not been investigated previously.

3.1.2 Tube viscometry and pulsed ultrasound velocimetry

In traditional tube viscometry pressure difference over a fixed distance of pipe and volumetric flow rate is used to determine the shear rheology. The concept of basic tube viscometry was used to develop the advanced Ultrasound Velocity Profiling (UVP) plus Pressure Drop (PD) system. Fluid flow in the pipes or capillaries over its length is caused by the pressure drop (ΔP) over the length (L) of the pipe. This relationship was first described by Hagen (1839) and Poiseuille (1840) independently, and

therefore is called the Hagen-Poiseuille law. The shear stress at the wall σ_w is determined by the pressure difference (ΔP) over a fixed distance of pipe (L):

$$\sigma_r = \frac{r\Delta P}{2L} \quad [3.2]$$

Equation [3.2] provides a measurement of shear stress at a single point of the capillary. Similarly, the shear rate at the wall is determined by flow rate Q as:

$$\dot{\gamma}_w = \frac{4Q}{\pi R^4} \quad [3.3]$$

where Q represents the volumetric flow rate (m^3/s).

The difference between a capillary and a pipe is that the diameter of the latter is much larger. In case of capillaries, the diameter ranges from 0.1-0.4mm, while pipes used in food application have diameters typically between 12-32mm (Steffe, 1996).

For simple Newtonian fluids, the rheology is determined based on the volumetric flow rate and the pressure drop over a fixed distance of pipe. This method, which is known as tube viscometry, enables determination of the shear viscosity at a single point in a capillary. To tackle the problem of single point measurements and to study non-Newtonian fluids, the parameter of Q, which provides the average velocity, has to be replaced by a method that determines the velocity profile over the entire cross-section of a pipe. Typically, the shear stress distribution in a pipe flow is represented by a straight line (Fig. 3). The velocity profile across a pipe diameter, $v(r)$, represents the instantaneous velocity distribution in a pipe diameter. The differentiation of velocity distribution at every radial position yields the shear rate distribution, as described in Eq. [3.1].

The apparent shear viscosity for a Newtonian fluid is calculated as;

$$\eta = \frac{\sigma}{\dot{\gamma}} \quad [3.4]$$

where η is the apparent viscosity, σ is the shear stress, and $\dot{\gamma}$ is the shear rate.

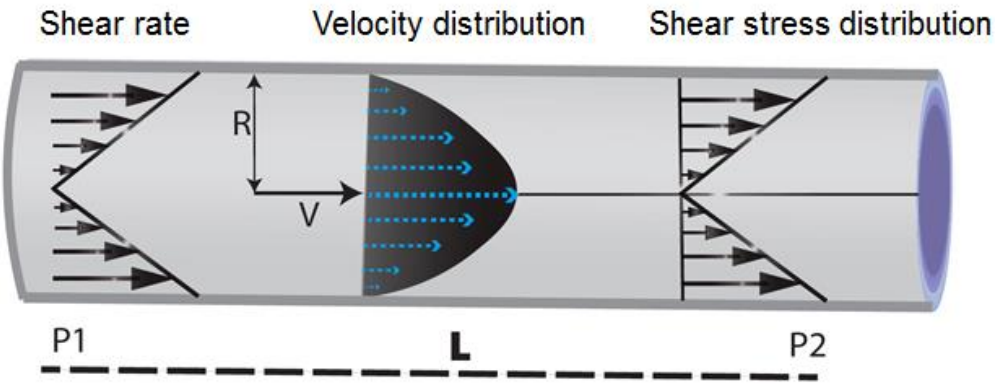

Figure 3: Fluid flow through a pipe under a laminar flow regime for a Newtonian fluid. It is clear from the figure that the maximum velocity is at the centre of the pipe (zero velocity at the wall), while the shear stress is maximum at the wall and zero at the centre of the pipe.

3.1.3 Flow characteristics of non-Newtonian fluids in pipes

Isaac Newtonian first observed that a shearing stress (σ) will cause a proportionally increasing deformation rate

$$\sigma \, \alpha \, \dot{\gamma} \quad \text{or} \quad \sigma \, \alpha \, \frac{dv}{dy} \qquad [3.5]$$

which is the relative change in the velocity (v) due to the applied shear force divided by the distance between the walls holding the fluid (y).

Removing the proportionality to introduce a constant (η),Eq. [3.5] becomes:

$$\sigma = \eta \, \frac{dv}{dy} \qquad [3.6]$$

Common examples of Newtonian fluids in food are water, honey, coffee, and carbonated beverages. In contrast to Newtonian fluids, non-Newtonian fluids do not follow Eq. [3.6], i.e., the relationship between the shear stress and shear rate is non-linear. Examples of non-Newtonian fluids are cosmetics, soap solutions, butter, jam, yoghurt, soup, and thickened fluids used for the treatment of dysphagia.

In the case of a non-Newtonian fluid, the flow properties can often be described using the Power-law model:

$$\sigma = K(\dot{\gamma})^n \qquad \text{or } \eta = K\dot{\gamma}^{n-1} \qquad [3.7]$$

where n is the flow index representing Newtonian (n=1), shear-thinning (n<1), and shear-thickening (n>1) fluids, and K is the consistency index. Figure 4 represents the velocity profiles of typical Power-law fluids flowing through circular tubes, under a laminar flow regime. A Newtonian fluid (n=1) will flow with a characteristic parabolic velocity profile, whereas shear-thinning fluids (n<1) have velocity profiles that are much flatter.

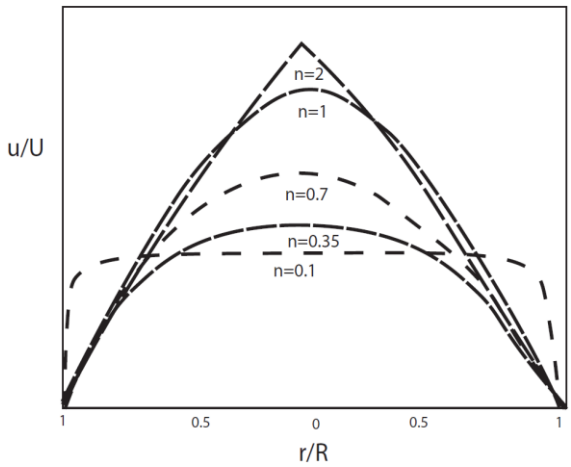

Figure 4: Shape of the velocity profile in a tube based on the Power-law model.

To calculate the shear rate and shear viscosity at radial position (r) for a Power-law fluid within a pipe, Eqs. [3.2] and [3.7] are combined and integrated:

$$\dot{\gamma} = \left(\frac{r\Delta P}{2LK}\right)^{1/n} \qquad [3.8]$$

$$\eta = K\left(\frac{r\Delta P}{2Lk}\right)^{1-1/n} \quad [3.9]$$

3.1.4 Ultrasound pulsed velocimetry+pressure-drop method for measuring shear viscometry

Ultrasound Velocity Profiling (UVP) is a technique that measures an instantaneous velocity profile in a fluid flow along the pulsed ultrasonic beam axis. The derivative of the measured velocity profile is used to determine the shear rate distribution across the beam axis. The average shear rate was determined with UVP for a bolus flow in this work. Ultrasound Velocity Profiling (UVP) can be combined with Pressure Drop (PD) measurements to determine rheological properties. The PD is used to determine the shear stress at the wall and the UVP+PD method is used to determine shear viscosity and yield stress measurements. Most of the work in this thesis is based on the UVP technique, except the work in **Paper II**, for which both the UVP and PD components are used.

The UVP technique detects the relative time lags between pulse emissions that are echoed by particles present in the fluid as a function of time. While the technique was originally developed to measure blood flow, it has been adapted to measure the flows of other fluids in research and engineering. The underlying principle is described in detail elsewhere (Takeda, 1995). A simplified schematic of the UVP technique is presented in Figure 5. An ultrasound transducer is mounted on a pipe of known length and diameter at an angle that ensures a measurable velocity component in the direction of the measuring line. The angle between the moving scattering particles and the inclination angle is called the 'Doppler angle'.

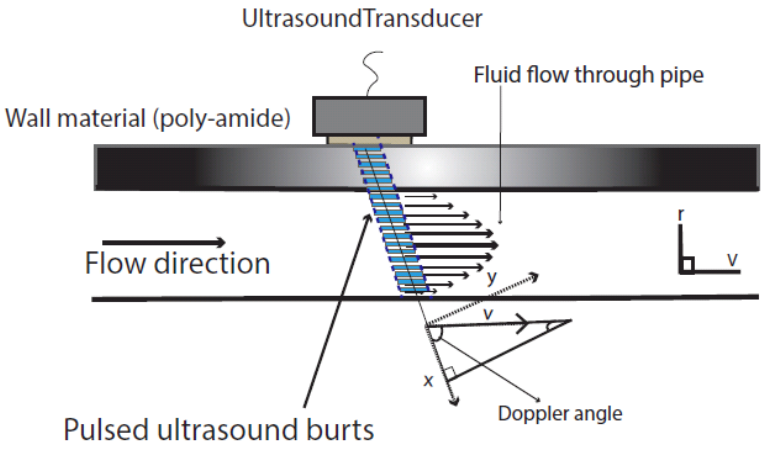

Figure 5: Schematic of the UVP method used to measure the velocity profile in the model pharynx.

The transducer emits a pulse train through the acoustic coupling and wall material into the sample fluid, which contains moving particles (or more precisely, micron-sized reflective surfaces) that are suspended in the flowing liquid (Fig. 5).

The echo that returns after collision with the moving reflectors in the fluid is sampled in a small time-window after each transmitted pulse. This small time-window is called a gate or a channel. A gate represents the range of widths from which the Doppler signals are acquired using a pulsed wave, while the width of each (w) channel is calculated from Eq. [3.10]:

$$w = c\frac{n}{2fo} \qquad [3.10]$$

where *w* is the width of the channel, *c* is the sound velocity (m/s), *n* is the number of cycles, and f_0 is the transmitting frequency (Hz). If the reflector is moving with a non-zero velocity into the ultrasound beam-axis there will be a shift in the position of the reflector between consecutive pulses. This shift is detected by the pulsed ultrasound system and is called a 'Doppler shift', although this is a matter of debate given that it is the shift in position of the reflector and not the shift in emitted frequency that is detected. This is discussed in detail by Jensen (Jensen, 1996). However, following convention, we use the term 'Doppler shift' in the present work. The Doppler-shifted frequency is determined by demodulation using time-domain or frequency-domain signal processing with the Incipientus ® equipment and the following expression:

$$fi^{Doppler} = \frac{2f_0 V_i cos\theta}{c} \qquad [3.11]$$

Meanwhile, the local velocity of the given fluid is determined by re-arranging Eq. [3.11] as follows:

$$Vz = \frac{c.fD}{2fo\cos\theta} \qquad [3.12]$$

where c is the ultrasound velocity, fD is the Doppler frequency shift, fo is the frequency emitted by the ultrasound transducer, and $\cos\theta$ is the Doppler angle.

The distance from the transducer face to the reflecting particle located along the given measuring line is determined by the time of flight as described in Eq. [3.13]. The time required for a pulse to reach the gate and return is converted into a physical distance, as described by the following equation:

$$S = \frac{c.t}{2} \qquad [3.13]$$

where *S* is the distance from the gate, *t* is the time interval, and *c* is the sound velocity. In this way, the velocities in space along the measuring line are calculated at multiple points, such that a complete velocity profile is established.

The velocity profiles in the current work are presented as Power spectra proportional to the energy of the Doppler-shifted signal. In the UVP method, only half of the velocity profile from the wall to the center of the pipe is required to calculate the rheological parameters (Fig. 6).

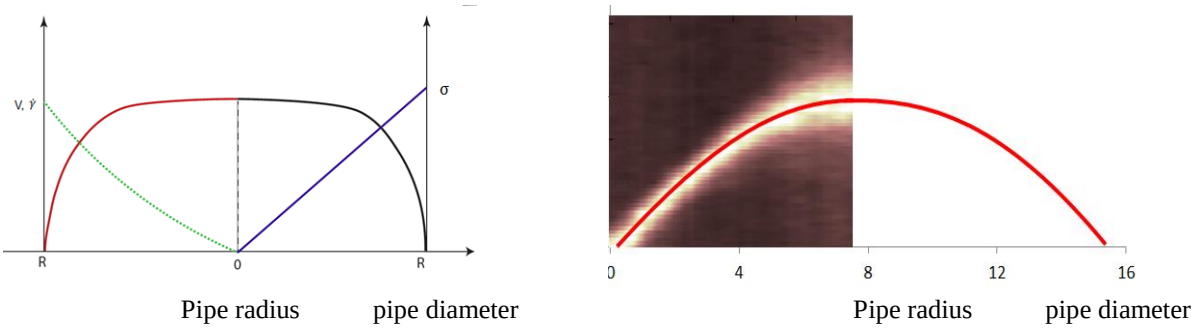

Figure 6: Schematic showing the flow of a typical shear thinning fluid. Schematic (left panel) further shows that half of the velocity profile is needed (from the transducer side) for shear rate determination (red line shows velocity and green line shear rate distribution). The secondary axis shows the shear rate distribution from the

wall to the centre of the pipe. The panel on the right shows the actual power spectra and the far side of the pipe where the velocity profile is assumed symmetrical.

Measurement artefacts in pulsed Doppler ultrasound (aliasing)

The term 'aliasing' refers to the artefact that is noted when the detected Doppler-induced frequency shift exceeds one-half of the instrument's Pulse Repition Frequency (PRF). In other words, the maximum detectable Doppler frequency shift is half of the PRF, i.e., $PRF=2_{fd(max)}$. In pulsed Doppler systems (but not in continuous wave Doppler), aliasing is an inherent artefact that occurs at high flow rates.

Aliasing results in the frequency shift (velocity profile) folding back into the lower regions of the frequency (Fig. 7), and it can be avoided by increasing the PRF to compensate for the higher frequencies.

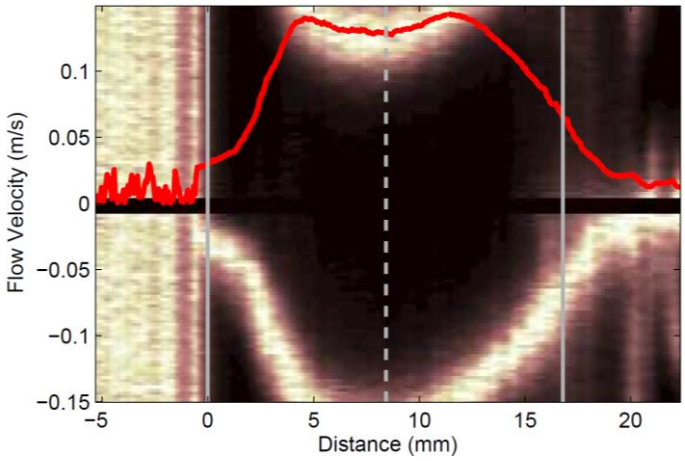

Figure 7: An example of an aliased velocity profile acquried at low PRF.

3.2 Extensional rheology

Besides their deformation under shear forces, fluids deform in the extension. Knowledge of extensional rheology is necessary for the processing and quality control of different products. Well-known examples of this for foodstuffs are flows through extruders or heat exchangers that involve an abrupt change in geometery accompanied by a sudden loss of water. Other examples where a food material undergoes extension include fibre spinning of soy proteins, dough sheeting, and finally bolus swallowing, as the food is squeezed between the back of the tongue and the palate. Therefore, extensional rheology is also considered in the present work. Mathematically, extensional viscosity can be defined as:

$$\eta_E = \frac{\sigma_E(t)}{\dot{\varepsilon}} \qquad [3.14]$$

Unlike shear, extensional viscosity is difficult to determine experimentally. Complications, such as shearing at the boundary, gravitational/inertial effects, and sample gripping, commonly arise. Various experimental techniques have been developed that are suitable for characterising from very-low-viscosity dilute solutions to very-high-viscosity polymeric melt materials. These techniques include: stagnation point flows; contraction flows; filament stretching; squeeze flow; fibre spinning; and Meissner extensional rheometry. The applicability of these techniques to different fluids at a range of zero shear viscosities is described in Figure 8 (Różańska, 2017). Zero shear viscosity is used here as a

reference to estimate the approximate point at which the given extensional rheology technique is applicable.

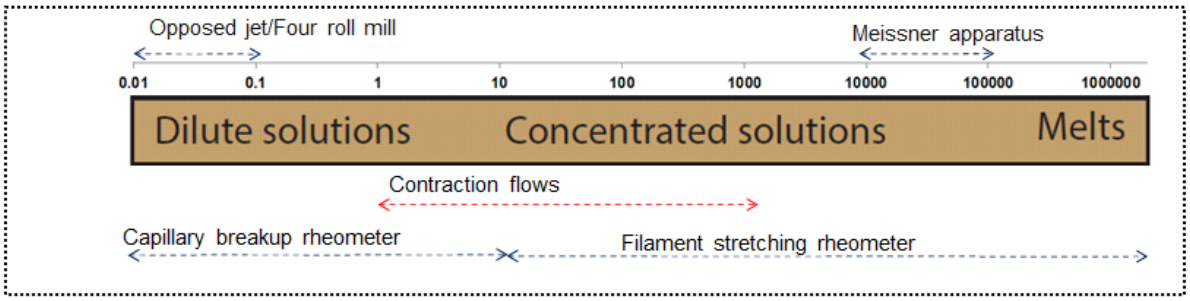

Figure 8: Range of zero shear viscosities at infinitely low deformation rates and the methods used for extensional viscosity measurements. The figure is adapted from (Różańska, 2017).

During "**stagnation point based flow**" the extensional deformation is evaluated in stagnation flows, which are normally created by colliding two jets at a 90º angle. Very high extension rates can be achieved at the stagnation point. The opposed jet technique and four-roll mill are examples of stagnation flow extensional viscosity measurement methods. In the **opposed jet technique**, two nozzles are aligned opposite to each other in a container that is composed of the fluid being tested. The sample is either pumped into or sucked out of the nozzle, so as to create a stagnation point around which the extensional flow takes place. The main drawback of stagnation point techniques is the lack of homogeneity of the flow. Pure extensional deformation is only possible close to the stagnation area, while shear flow predominates along the nozzle. **Contraction flow** techniques, such as the Hyperbolic Contraction Flow (HCF) used here, are based on creating a fluid flow through an abrupt contraction as presented later in Figure 10. The pressure drop and flow rate are measured as the fluid flows through the orifice. This technique is ideal for fluids of medium viscosity.

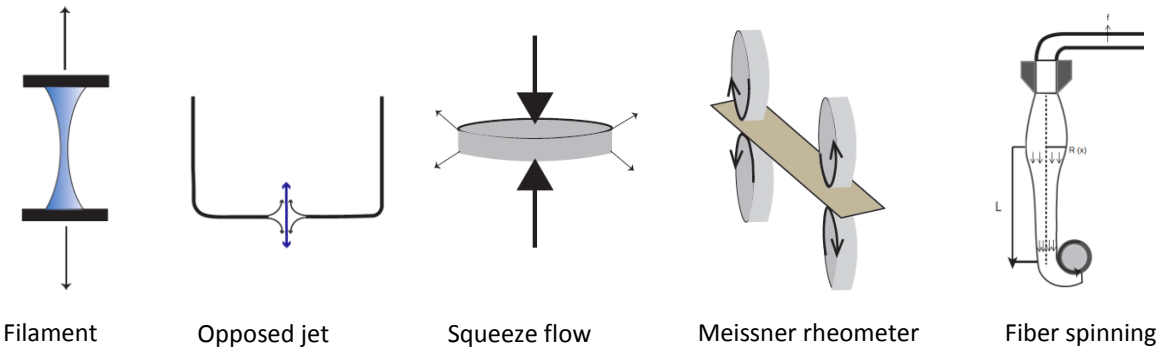

Figure 9: Illustration of the techniques used to measure extensional viscosity

In the **filament stretching technique**, a filament is created from the sample being tested by placing the sample between two parallel plates. The lower plate remains stationary, while the upper plate is raised rapidly to stretch the sample. During the measurement, the change in filament diameter is monitored with a high-speed camera or laser. For the filament technique to be effective, the sample must be viscous and sufficiently sticky to be stretched. The Capillary Breakup Extensional Rheometer (CaBER), as mentioned briefly in this study, is one example of filament stretching. In the **squeezed flow** technique, the cylindrical plate is placed between two plates and squeezed, so as to create a biaxial extension. A limitation of the technique is that only $\varepsilon_H \approx 1$ is applicable due to a high level of

friction. Another technique for measuring extensional viscosity is the **Meissner extensional rheometer**, in which the sample is stretched by two sets of oppositely rotating toothed belts, ensuring a constant extension rate and ε_H=7. The stress applied is recorded on one set of rollers, while the extension rate is recorded with a video camera. Detailed discussions of these techniques can be found in a previously published review (Kocsis, 1995). The HCF and CaBER methods used in this study are briefly discussed below.

During **fibre spinning**, the sample being tested is deformed based on its spin-ability, e.g., the spin-line rheometer shown in Figure 9. The fluid that is passing through a thin-walled tube is pumped from a nozzle mounted at the end of the thin-walled tube. The fluid filament is elongated by a rotating drum. During this process, the force exerted on the thin-walled tube is calculated based on how much this tube has deflected. Elongation of the filament is photographed, which serves as the basis for calculating the extension rate. The draw-back of fibre spinning is that only low-viscosity samples are measurable (1-10 Pa.s) (Różańska, 2017).

3.2.1 HCF technique

In the HCF technique for extensional viscosity measurements, a hyperbolically shaped nozzle (Fig. 10) ensures steady-state extension of the given fluid.

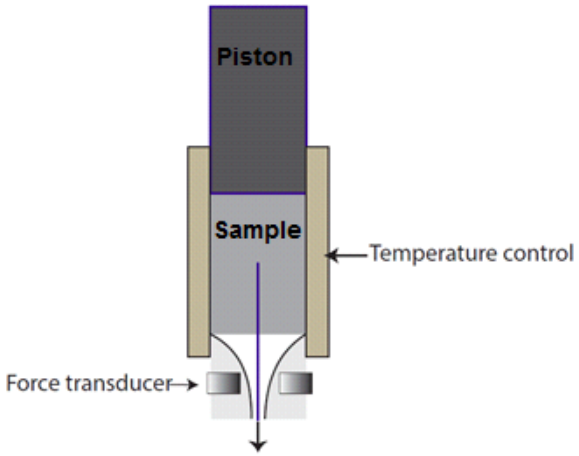

Figure 10: Illustration of the hyperbolic contraction flow nozzle.

This technique was first utilized by David James (James, 1991), while Leif Bohlin (Bohlin, 1999) presented an analytical solution for David Bindings analysis of the extensional flow of a Power-law, and designed a measuring system that contained a hyperbolic nozzle (Binding *et al.*, 1989).

Assuming a Power-law fluid, $\sigma = K\dot{\gamma}^n$, the constant extension rate throughout the nozzle (Fig. 11) is given by:

$$\dot{\varepsilon} = -2\frac{3n+1}{n+1}\frac{Q}{\pi r^3}\frac{dr}{dz} \qquad [3.15]$$

This constant extension rate has been confirmed by others (Nyström *et al.*, 2017).
While the radius of the nozzle (Fig. 11) at any point *Z* along the height of the nozzle (*H*) is expressed (Wikström & and Bohlin, 1999) as:

$$r(z) = \frac{r_0}{\sqrt{\frac{z}{H}.\left[\frac{r0^2}{r_1^2}\right]+1}} \qquad [3.16]$$

where r_0 and r_1 are the inlet radius and outlet radius, respectively, of the hyperbolic contraction nozzle, and H is the height of the nozzle.

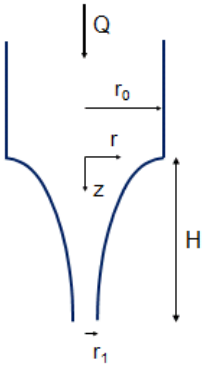

Figure 11: Illustration of the contraction nozzle. Taken from (Wikström & Bohlin, 1999)

During contraction flow beside involving extension, a fluid will also experience shear, which is calculated as (Wikström *et al.*, 1999):

$$\sigma_{shear} = \frac{4H\left(3+\frac{1}{n}\right)^n\left(\frac{K}{\pi}\right)^n(\pi r o^2 v)^n\left(\frac{1}{r0^{3n+1}}\right)\left[\left(\frac{r0^2}{r1^2}\right)^{\frac{3n+3}{2}}-1\right]}{(3n+3)\left(\frac{r0^2}{r1^2}-1\right)} \qquad [3.17]$$

The final extensional viscosity, reported as the corrected extensional viscosity, is obtained by subtracting the shear stress contribution in the HCF nozzle from the ratio of stress σ measured by the load cell (F/A) to the rate of extension

$$\eta_e = \frac{\sigma_{measured} - \sigma_{Shear}}{\dot{\varepsilon}} \qquad [3.18]$$

3.2.2 Measurement of extensional properties using capillary break-up

Extensional deformation can be measured with CaBER. The technique is based on monitoring the dynamics of a fluid thread during short-duration, rapid deformation. The deformation results in necking and an unstable geometric shape of the fluid element. This unstable fluid shape is allowed to relax and break apart under capillary forces. The extensional stress in the fluid resists the filament break-up, which is characteristic for a given fluid. To monitor the changes in filament diameter over time at the mid-point, $D_{mid}(t)$, a laser micrometer targeted at the centre of the filament is used.

The Hencky strain in CaBER is measured from the logarithmic evolution of the mid-point diameter over time with respect to the original diameter:

$$\varepsilon_H = 2\ln(D_0/D_{mid}(t) \qquad [3.19]$$

To obtain the extensional viscosity in the CaBER, the following relation is used:

$$\overline{\eta}_{app}(\varepsilon) = \frac{2\sigma/D_{mid}(t)}{\left[\frac{-2}{D_{mid}}\frac{d\,D_{mid}}{dt}\right]} = -\frac{\sigma}{\frac{d\,D_{mid}}{dt}} \qquad [3.20]$$

In the equation, the σ term represents the surface tension, which cannot be measured directly in the CaBER and therefore has to be measured separately and inputted to the software; the terms shown in brackets represent the extension rate $\dot{\varepsilon}(t)$.

The results obtained from the CaBER are often represented as the normalised logarithmic diameter $D(t)/D_0$ recorded during thinning as a function of time (s), where D_0 is the filament diameter at time zero and D(t) is the change in filament diameter over time. Figure 12 shows a typical example of how a Newtonian syrup filament diameter evolves over time.

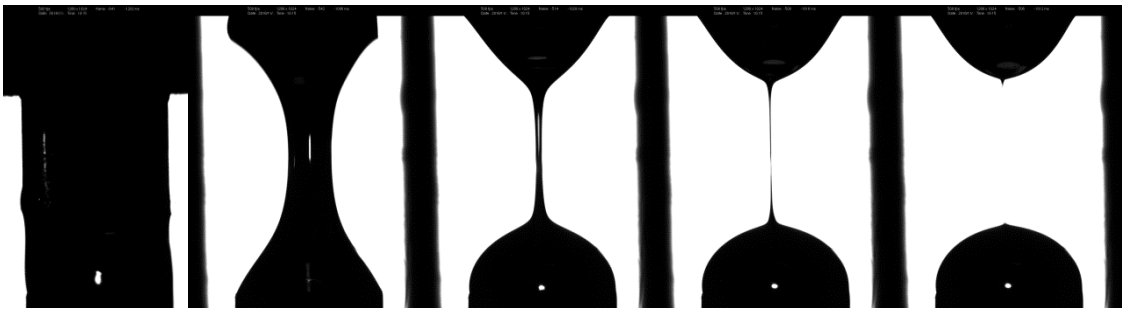

Figure 12: Schematic of filament evolution in the CaBER: (a) loaded; (b) during stretching; (c) shortly after stretching is stopped; (d) during capillary drainage; and (e) after breakup of the Newtonian syrup with 0.55 Pa.s of shear viscosity.

3.3 Physiology of swallowing

Normal swallowing involves rapid transport of food or liquids from the mouth towards the stomach, where the goal is to guide the food safely towards the stomach without entrance into the airways. Swallowing consists of four stages: the oral preparatory stage; the oral stage; the pharyngeal stage; and the oesophageal stage (Bulow, 2003; (Nishinari *et al.*, 2011). Twenty-eight different muscles are involved in the transport of a bolus from the oral cavity to the oesophagus (Ekberg, 1997). These muscles ensure that the bolus does not enter the airways.

3.3.1 Oral Preparatory stage:

The oral preparatory stage, which is also called the bolus-forming stage, starts with the sight or smell of the food. In this stage, food/drink received by the mouth is masticated and mixed with saliva in order to form a **bolus**, which has a consistency that makes it readily swallow-able. The posterior of the tongue and the soft palate ensure that the food does enter the pharynx prematurely. The cheek muscles restrict lateral movement of the food, while the lips prevent the frontal escape of the food from the mouth. Normal breathing continues at this stage of swallowing (Bulow, 2003).

3.3.2 Oral stage:

In this stage, the bolus is displaced backwards by the tongue toward the pharynx (Fig. 13). The tongue executes the pushing function through a stripping action against the hard palate. This promotes the posterior mobility of the bolus towards the pharynx. The oral stage terminates when the bolus reaches the back of the tongue close to the faucal arches.

3.3.3 Pharyngeal stage:

This is the first involuntary stage of swallowing. It starts with the activity of the hyoid bone. The hyoid bone starts to move upwards and forward. This helps to expand the pharynx, resulting in the pharynx adopting an elliptical shape as it receives the bolus. The epiglottis tilts back and down, to seal off the airways and to prevent the entrance of food into the airways, which means that breathing is stopped momentarily. Once the pharyngeal cycle is over, the hyoid bone returns to its original position (F. J. Chen *et al.*, 2012). As the pharynx is partly shared by the airways and food-swallowing tract, a misdirected bolus can enter the airways, resulting in aspiration. Thus, the pharyngeal stage of bolus transport is the most crucial. Nevertheless, it is relatively poorly studied, especially during *in vitro* modeling, as compared to the oral and esophageal stages.

3.3.4 Esophageal stage:

This is the final stage of swallowing. Similar to the pharyngeal stage, the stage is involuntary. It starts at the upper esophagus sphincter where the bolus enters. The peristaltic action on the bolus of the circular muscles pushes the bolus slowly downwards to the lower oesophageal sphincter, and thereafter towards the stomach (F. J. Chen *et al.*, 2012; Yang *et al.*, 2007); Bulow, 2003)

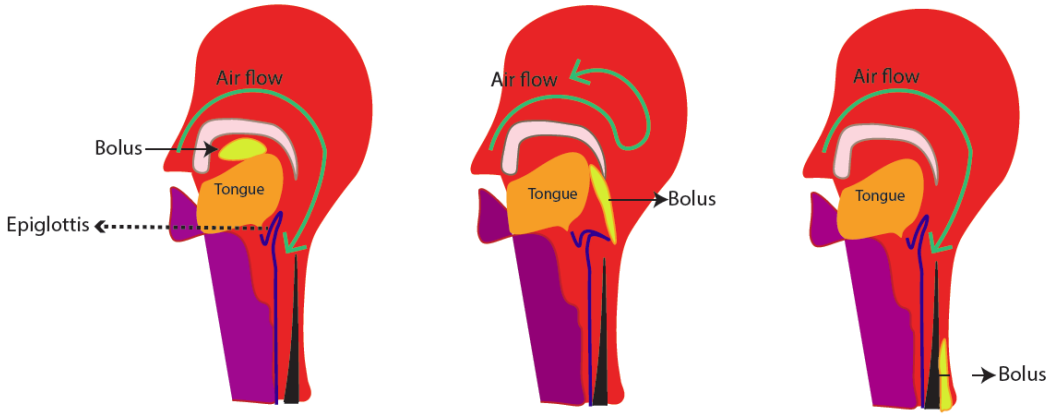

Figure 13: Voluntary and involuntary stages of swallowing: the oral, pharyngeal, and oesophageal stages (left to right). Note the position of the epiglottis and movement of the bolus during the different stages. The arrow indicates the air flow regulation during the different stages.

4. RHEOLOGICAL AND MICROSTRUCTURAL PROPERTIES OF THE MODEL FLUIDS AND FOOD THICKENERS

Texture modification through increasing bolus viscosity is one of the most common type of intervention in dysphagia management (Tobin *et al.*, 2017). Other rheological properties, such as bolus elasticity (bolus cohesion), yield stress (level of force needed to initiate the flow), and the microstructural description of the flow of thickened fluids have been studied to lesser extents. Therefore, this section is mainly concerned with characterising the starch- and gum-based thickeners for extensional rheology, and yield stress, and with understanding the microstructural features responsible for rheological properties (**Paper II**). As a starting point to model the pharynx, the UVP method was used for fluid flow visualisation, to study the in-line rheology and compare it with the traditional laboratory-based rheometry. The measured fluids were both model fluids and those thickened with powders for dysphagia management (**Paper II**).

4.1 Materials

Five commercial thickeners and three model fluids were characterised for: shear viscosity (using the UVP-PD method and laboratory-based viscometry), microstructure, and extensional viscosity. The thickeners come in two major formulations: gum-based and starch-based. The gum-based thickeners were: Nutilis (Nutricia Nordic AB, Stockholm, Sweden); Nestlé Clear (Nestlé Health Science Centre, Stockholm, Sweden); and Fresubin Clear (Fresenius Kabi GmbH, Bad Homburg, Germany). The starch-based thickeners were: Nestlé Thicken-up (Nestlé Health Science Centre); and Findus thickener (Findus Sweden AB, Malmö). To make the relevant comparisons, the viscosities of the two major classes of thickeners (gum-based and starch-based) were set to be always within the range of Honey consistency (0.351–1.750 Pa.s) on the NDD scale, and more specifically, 0.55±0.03 Pas at50 s-1, which is the shear rate that is believed to govern the oral and pharyngeal swallowing stages.

Model fluids, which are fluids of known composition, serve as references to distinguish between, for example, pure elastic and pure viscous effects. In the current project, three model fluids (Newtonian, Boger, and shear-thinning) were created. Similar to the thickeners, the consistencies of the model fluids were set at 0.55 Pa.s at a shear rate of 50 s^{-1}. The Newtonian fluid used in **Paper II** was based on a diluted syrup, called Lys syrup (84% sugar; (Dansukker, Malmö, Sweden). The Boger fluid used in **Paper II** was prepared by dissolving a small amount (150 ppm) of pre-dissolved polyacrylamide (PAA) in diluted syrup, while the shear-thinning fluids (**Paper II**) were made from either PAA or xanthan gum by dissolving the respective polymers in water to the appropriate consistency (Table 1). The xanthan gum used in this study was Grinsted Xanthan CLEAR 80 (Danisco France SAS, Melle, France), and the PAA was supplied by ACROS Organics (Geel, Belgium).

Procedure for preparing the model fluids (Paper II)

The model Newtonian, Boger, and shear-thinning fluids were made by diluting the syrup with water to the targeted viscosity of 0.55 Pa.s at a shear rate of 50 s^{-1}. In the cases of the Boger and shear-thinning fluids, mixing with a concentrated solution of either the xanthan gum or PAA polymer (Table 1) was performed for 48 hours at room temperature (23°C) until the samples were completely dissolved.

Procedure for preparation of commercial thickeners in water

A large volume of the thickener solution (~2 L) was mixed with tap water according to the manufacturer's guidelines to achieve a honey-like consistency, and agitation was applied with a magnetic stirrer until the thickener was completely dissolved (about 1 hour). The amount of powder that was added to the water to achieve a viscosity of 0.55±0.03 Pa.s at a shear rate of 50s^{-1} is listed in Table 1. In general, the thickeners were highly soluble in water.

Table 1: Amounts of thickeners added to achieve a viscosity of approximately 0.55 Pa.s at a shear rate of 50 s-1.

Thickener	Amount (g) of thickener added[1] to achieve a viscosity of ~ 0.55 Pa.s at shear rate of 50 s^{-1}	Thickening agent(s)
Nutilis	4.0	maltodextrin, modified starch, xanthan gum, guar gum
Fresubin Clear	4.0	modified starch, xanthan, maltodextrin, modified cellulose
Nestlé Thicken-up	5.15	modified maize starch
Nestlé Clear	5.7	maltodextrin, xanthan gum
Findus	25.0	maize starch
Newtonian fluid	-	-
Boger fluid	150 ppm	PAA
Shear-thinning fluid	2%	xanthan gum

[1]*During preparation of the different batches, a standard deviation of ±0.05 g was noticed. Units other than grams are designated in the table.*

4.2 Light and electron microscopy

Light Microscopy (LM) and Transmission Electron Microscopy (TEM) were used to analyse the structural properties of the starch-based and gum-based thickeners (**Paper II**). LM was the preferred technique for analysing the starch-based thickener owing to its larger granular size. Starch granules typically swell during hydration, thereby increasing the contributing to the viscosity of the material. Swollen starch granules can be stained with iodine and visualised by light microscopy upon hydration. However, since the structure of xanthan-gum is too fine to be viewed under LM, a more sensitive technique, such as TEM, is required. TEM is an electron-based technique. Electrons, which have shorter wavelengths than light, provide better resolution, typically up to 5×10^{-10} m. Unlike LM, TEM requires a controlled environment, as under normal atmospheric conditions the electrons react with ordinary gases in the air. Therefore, TEM is carried out under a vacuum, with measures taken to ensure that the sample does not evaporate. This means that the sample has to be prepared prior to analysis using well-controlled preparation techniques that do not alter the sample structure. The

preparation technique used here was freeze-fracture replication. The procedures used for the performance of LM and TEM are described below.

Procedure for LM visualisation

The solutions were analysed both as a solution and dried on an objective glass on a heating stage set at ~40°C. The staining solution was either added to the solution and analysed or added to the dried film of the solution on the objective glass. Staining involved the addition of Lugol's iodine solution or a 1:1 mixture of Lugol's iodine and Light Green solution. Lugol's iodine stains amylopectin a pink-to-brownish colour and stains amylose purple. Lugol's iodine stains proteins yellow, while Light Green stains proteins green, which makes the latter more suitable for protein visualisation. The staining solutions were added to the samples and a cover glass was placed on top. The cover glass was sealed to the objective glass with nail polish, to prevent evaporation of the iodine. Differential Interference Contrast (DIC) was used to enhance visualisation of the interfaces. The LM used a Nikon Microphot-FXA microscope (Nikon, Tokyo, Japan), equipped with an Olympus Altra 20 colour camera connected to a computer and operated using the Olympus Cellsens Dimension software (Olympus Soft Imaging Solutions, Münster, Germany).

Procedure for TEM visualisation

Three different xanthan-based thickeners were analysed using the mica sandwich freeze-etching preparation method, in which 7 µl of a thickener (diluted to the appropriate concentration) were placed between two newly cleaved mica sheets. The sheets with the sample were placed together as a sandwich and then rapidly frozen by immersing the mica sandwich in liquid nitrogen. The mica sheets were separated under liquid nitrogen, and one of the sheets with a thin layer of the sample was quickly transferred to a vacuum chamber that contained a pre-cooled Balzers freeze-etching unit at -170ºC (Balzers BAF 400; Balzers Union Aktiengesellschaft, Balzers, Liechtenstein). When a vacuum was created in the chamber the temperature was increased to -90ºC and the sample was left for 2 hours for the water to sublimate. A metal replica of the sample was created by shadowing a ~0.8-nm-thick layer of platinum at an angle of 6º, followed by shadowing a ~20-nm-thick layer of carbon at an angle of 80º on the surface of the sample. The thickness of the metal replica was controlled by a quartz crystal monitor. Only the platinum layer gives contrast in the image, while the carbon layer is a support for the very thin metal layer when it is analysed using TEM. The replicas were then removed from the mica sheets and cleaned from the sample by immersing them first in deionised water followed by H_2SO_4 (70%) and several washes with deionised water. Prior to the TEM analysis, the samples were placed on copper grids. The TEM used for analysing the replicas was the LEO 706E (LEO Electron Microscopy Ltd., Cambridge, England), which was operated at an accelerating voltage of 80 kV.

4.3 Results and discussion on the rheological properties and microstructure

In the following sections, the rheological properties of the thickeners and model fluids are briefly described, while the thickeners are also evaluated by microscopy to understand the structural differences that determine the rheological properties.

4.3.1 Shear viscosity

The procedure that was followed to measure the steady-state flow curves is described in **Paper II**.
The gum-based thickeners were found to be more shear-thinning (Fig. 14; upper panel), with flow curves that were steeper than the starch-based thickeners. The Power-law flow index (*n*), which is an indicator of the degree of shear-thinning, supports this finding, as presented in **Paper II**. Nestlé Clear

and Fresubin Clear are shear-thinning to the same extent, with *n*=0.19 for both thickeners, followed by Nutilis, with n=0.33. In comparison, starch-based thickeners are less shear-thinning, with *n*=0.39 for Nestlé Thicken-up and *n*=0.61 for Findus thickener, respectively. Figure 14 shows the flow curves for the model PAA- and xanthan gum-based shear-thinning agents, Boger fluids (PAA-based), and the corresponding Newtonian fluid (composed of syrup). The Newtonian fluid shows its characteristic rheological property, in that its viscosity is independent of the applied shear rate (*n*=1), as is evident in Figure 14 (lower panel) with Power-law index *n*=~1. In contrast, the Boger fluid demonstrates the expected independence of viscosity in relation to shear rate (*n*=0.98). The main difference is when the two fluids are characterised by large-scale deformation, as discussed in the next section.

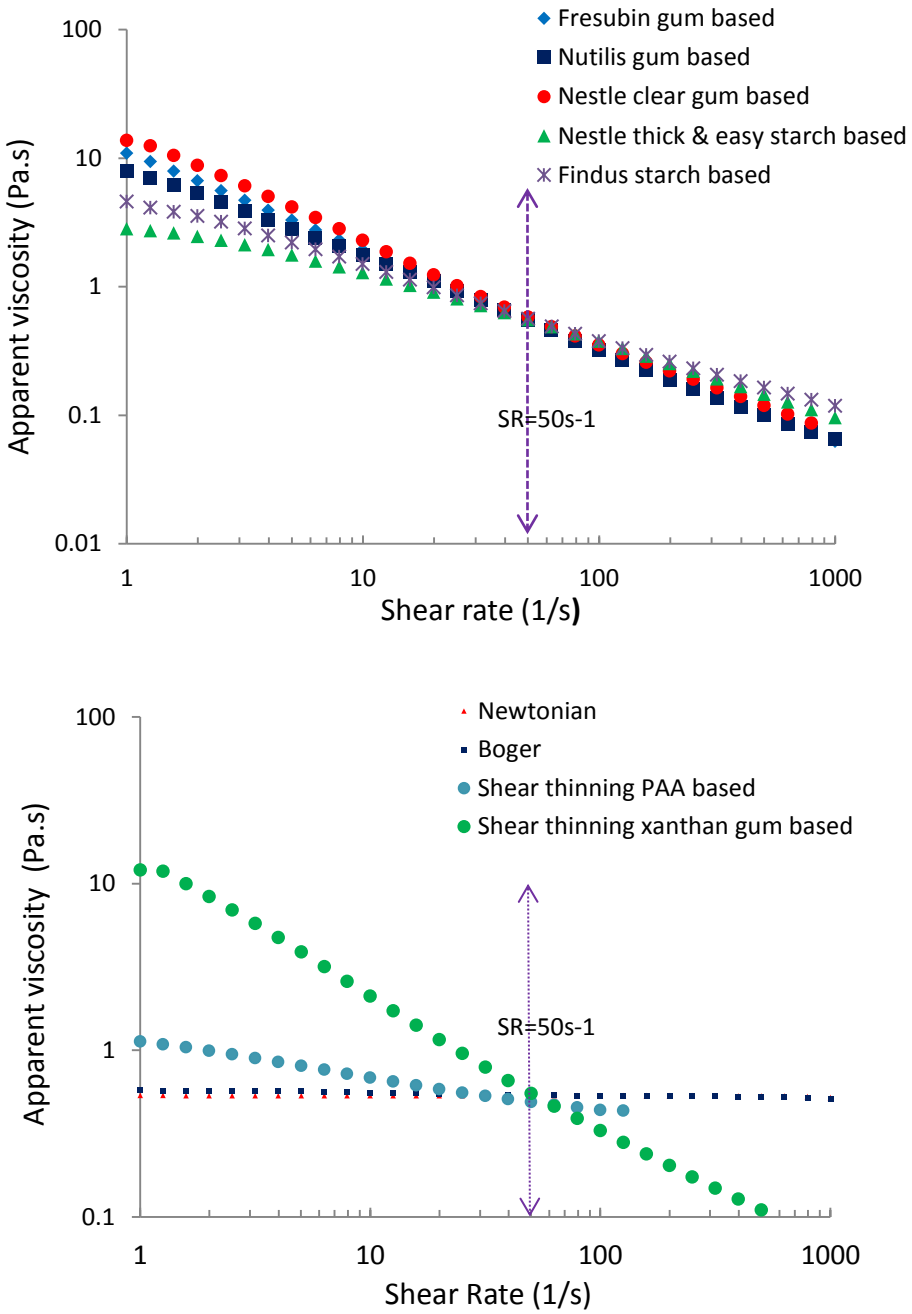

Figure 14: Flow curves of the thickeners used for dysphagia management (top panel) and of the model fluids (bottom panel). The viscosities of all the fluids are set to ~0.55±0.03 Pa.s at a shear rate (SR) of 50 s^{-1}.

There was slight shear thinning of the Boger fluid at very low shear rates, which occurred due to adjustments to the initial polymer structure, as also noted in previous studies (Anne Laure Koliandris, 2010). Of the two shear-thinning model fluids, the xanthan gum-based fluid was more shear-thinning (n= 0.22) than the model PAA-based shear-thinning fluid. The model fluids used here mainly serve as references, as they have standard compositions and known rheological behaviours. This helps to eliminate any effects from other ingredients used in thickened fluids. Model fluids were used in **Paper I** to study the relationship between elasticity and safe swallowing in patients. Moreover, the PAA used in this study was not food-grade, and so is not of any immediate direct value. The use of PAA in this work was primarily motivated by its high-level elasticity. Even though it was added in a small amount, the PAA induced highly elastic effects. This allows thickener manufacturers to define where the currently used elastic polymer, xanthan gum, resides on the elasticity scale. In the future, we expect fluid elasticity to become a key factor (in addition to shear viscosity) when designing diets for persons with dysphagia. Therefore, food industry needs to have the possibility to develop new ingredients with equivalent rheological properties. The structures and rheological features of the PAA- and xanthan gum-based thickeners are described in detail in the next section.

Thickeners have traditionally used starch as the viscosity-enhancing ingredient, due to its easy dissolution and low cost. Starch-based thickeners, however, have the inherent disadvantage of susceptibility to amylase action during oral processing, which may reduce their viscosity (Leonard *et al.*, 2014).

4.3.2 Extensional viscosity in HCF

As proposed in **Paper 1**, elasticity exerts an influence on safe swallowing. Therefore, all the thickeners used in dysphagia management were characterised in terms of extensional rheology using the HCF technique (Fig. 15). The extension rate was varied from 1 s^{-1} to 100 s^{-1}. In general, the thickeners composed of xanthan gum were more elastic than the ones that have starch as the thickener. Furthermore, both the gum-based and starch-based thickeners behaved as extension-thinning fluids, which does not accord with what is expected for a typical shear-thinning polymer in large-scale deformation. A material that is shear-thinning often behaves as an extension-thickening, although it is not a rule of thumb (H.A. Barnes *et al.*, 1997). The behaviour of the polymer is largely dependent upon the technique used for measurement. The theory states that polymer molecules that are originally in coiled form, when added to a solution, become stretched out and aligned in the direction of the flow. As the polymer molecules become aligned in the flow direction, they offer less resistance to shear deformation, which is manifested as a shear-thinning behaviour. Similarly, the same polymer molecules when stretched out (extensionally deformed) will align in this direction, as they are now deformed in extension mode, such that the resistance to extensional deformation increases, i.e., the extensional viscosity increases with increasing deformation rate, as noted here.

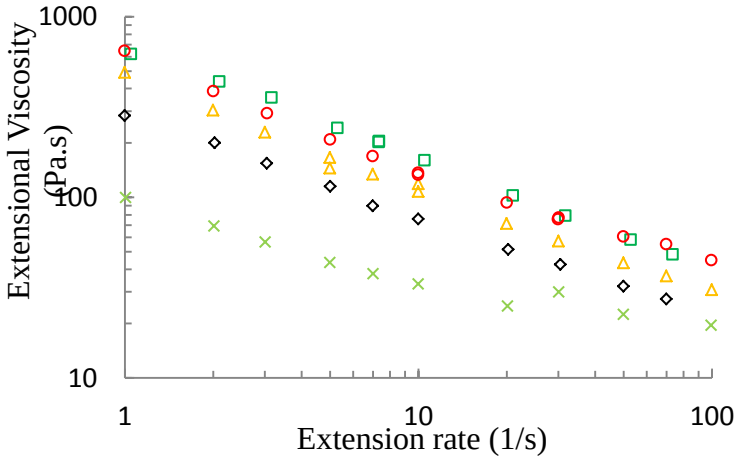

Figure 15: Extensional viscosities (Pa.s) of thickener-based dysphagia-management aqueous solutions for different extension rates: Fresubin Clear □; Nestlé Clear ○; Nutilis △; Nestlé Thicken-up ◇; and Findus thickener ×.

A similar extension-thinning behaviour was observed for the model xanthan gum fluid, which was dissolved in water and deformed extensionally (Fig. 16). Therefore, in the HCF method, a xanthan gum-based thickener exhibits extension thinning. The Trouton ratio ($Tr = \frac{\eta_e}{\eta}$) was considered for the fluids characterized here. The T_r was non-dimensionalised as: K*/K, where K* and K are the consistency indices under extensional deformation and shear deformation, respectively. The non-dimensionalised values for the gum-thickened fluids were in the order of: Nutilis powder (T_r=57); Nestlé Clear (T_r=45); and Fresubin Clear (T_r=41). Similarly, the Trouton ratios for the starch-thickened fluids were: Nestlé Thicken-up (T_r=43); and Findus thickener (T_r=40). One would expect the Trouton ratios to be much higher for the more-elastic gum-thickened fluids. However, application of the T_r is valid only at low extension rates; the ratio may not give accurate results at higher extension rates, as discussed previously (Petrie, 2006). Similarly, the Trouton ratio is dependent upon the technique used for the measurement and the extension rates. The HCF technique is not suitable for predicting T_r when sufficiently low extension rates are not achievable.

One of the primary aims of this thesis was to observe the effect of elasticity on safe swallowing in patients with dysphagia using a fluid that is purely elastic in nature. Food-grade polymers that provide high-level elasticity are scarce, and the most well-known thickener is xanthan gum, which was used in the clinical study described in **Paper 1**. Non-food-grade ingredients, such as PAA, can be used in much lower concentrations to create a Boger fluid with elasticity that is many times higher. Thus, only 150 ppm (0.015%) PAA needed to be dissolved in syrup to create a highly elastic Boger fluid (Fig. 16), while 0.2% PAA was used to create even more potent elastic effects and shear-thinning behaviours during experiments with shear deformation.

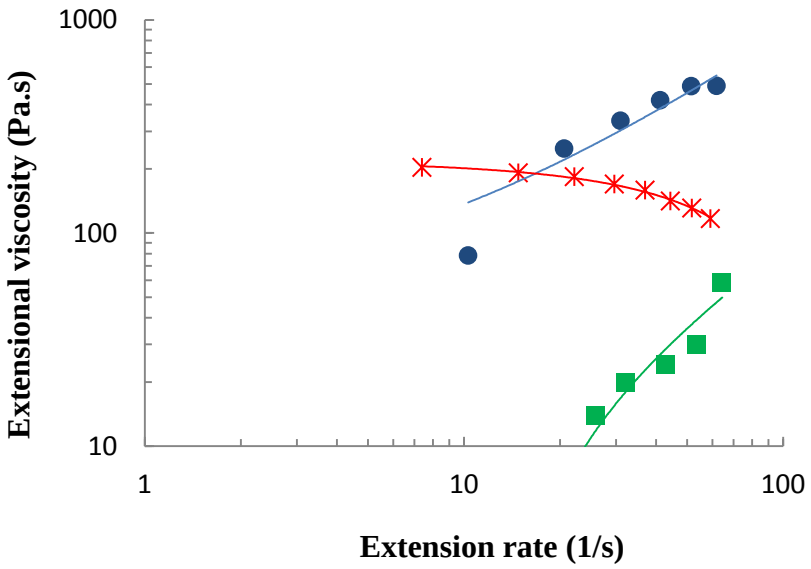

Figure 16: Apparent extensional viscosities of the model fluids: Boger □ (0.015% PAA in syrup); shear-thinning food-grade ✳ (2% xanthan gum in water); and shear-thinning non-food-grade ○ (0.2% PAA in syrup).

In contrast to the extension-thinning behaviour seen for the model xanthan gum fluids and the thickeners with the same polymer, extension-thickening behaviours were observed for the PAA-based model fluids. These results are consistent with the results in the literature (Ferguson *et al.*, 1990). The two polymers behave differently during large-scale deformation due to differences in their structural architectures. Xanthan gum is in the form of a rigid rod, while PAA is a coiled polymer. The rigid, rod-like conformation of xanthan gum results in faster alignment in the extensional direction. As a consequence, xanthan gum offers less resistance in extension at high extension rates, and thus shows an extension-thinning behaviour. In contrast, PAA behaves as an extension-thickening agent due to its coiled structure, which means that the polymer requires greater strains to uncoil and align it in the stretching direction (Ferguson *et al.*, 1990). This shows that extensional deformation provides a better explanation for the structural properties of large, complex polymers. To complement the elastic properties seen in HCF, CaBER was used, as mentioned below.

4.4 Yield stress and microstructural properties

Certain materials exhibit solid-like behaviours unless a finite stress, called 'yield stress', is applied to achieve a flow. Typical examples of yield stress fluids in the food industry are mayonnaise and ketchup. A fluid that has a yield stress (T_y) is believed to promote internal binding of the bolus, thereby maintaining the integrity of the bolus during pharyngeal swallowing such that bolus disintegration is avoided during flow (Marcotte, 2001; Steele *et al.*, 2014). This property of yield stress is more important in individuals who are suffering from dysphagia. Therefore, the two major classes of thickeners (gum-based and starch-based) were analysed for their yield stress properties. A fluid that has a T_y flows with a characteristic plug velocity profile in the centre of the pipe. The diameter of this plug is proportional to the yield stress of the fluid (Fig. 17).

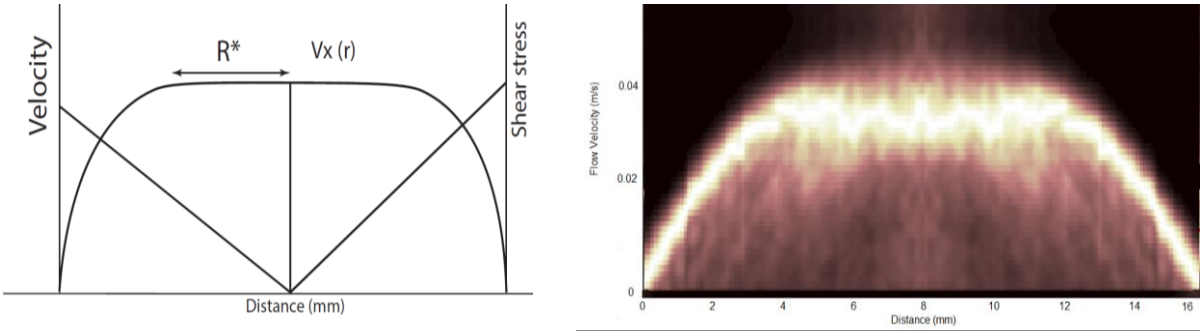

Figure 17: Yield stress measurement using the PUV+PD method, obtained from the plug of the velocity profile in the fluid flow and pressure drop. The right panel shows the actual yield stress measured by the UVP+PD method.

The velocity profiles obtained when pumping different fluids and conducting UVP+PD measurements can be used to estimate the characteristic yield stress value as:

$$\sigma_0 = \frac{\dot{R}\Delta P}{2l} \qquad [4.1]$$

where ΔP is the pressure drop across the pipe length (l), and $\dot{R}$ is the radius of the plug for a given fluid.

The yield stress values for the thickened fluids measured with the UVP+PD method were compared with the values measured with a stress-control rheometer, Reologica StressTech HR (Reologica Instruments AB, Lund, Sweden) (Table 2). Details of the method followed are provided in **Paper II**.

Table 2: Yield stress values for the thickener measured with PUV+PD and the Reologica Stresstech rheometer

Sample name	UVP PD (Pa)	StressTech (Pa)	Composition based on:
Fresubin Clear	13.5±0	11.83±0.24	Xanthan gum
Nutilis	4.43±0.37	2.23±0.97	Xanthan gum
Nestlé Clear	10.83±4.05	12.05±0.07	Xanthan gum
Nestlé Thicken-up	0	0	Starch
Findus thickener	1.87±0	0	Starch

Our results show that the samples with xanthan gum have a mild yield stress, with the highest values seen for Fresubin Clear and Nestlé Clear (T_y=~12, StressTech), followed by Nutilis (T_y =~2, StressTech). For the starch-based thickeners, the yield stress value was found to be negligible using the two methods for measuring T_y.

To understand why the gum-based thickeners show a yield stress and the starch based-thickeners do not, microstructural analyses were performed using LM and TEM. The acquired images are shown in Figure 18. The xanthan gum-based thickeners of Fresubin Clear (Fig. 18 A), Nestlé Clear (Fig. 18 B), and Nutilis (Fig. 18 C) formed transparent solutions, which meant that no microstructure could by detected by LM due to the limiting resolution of about 1 mm. To visualise the main structural component, i.e., xanthan gum, TEM was used. As electrons have a shorter wavelength than ordinary light, they provide better resolution than LM, typically to the nanometre scale. In the TEM analysis, a

meshed network structure was observed for all the xanthan gum-based thickeners (Fig. 18 A-C). This meshed structure probably is the reason for the minor yield stress seen for xanthan gum-based thickeners, and it was not present in the starched thickeners (Fig. 18 D and E). The starch-based thickener was too heterogeneous to be studied using TEM.

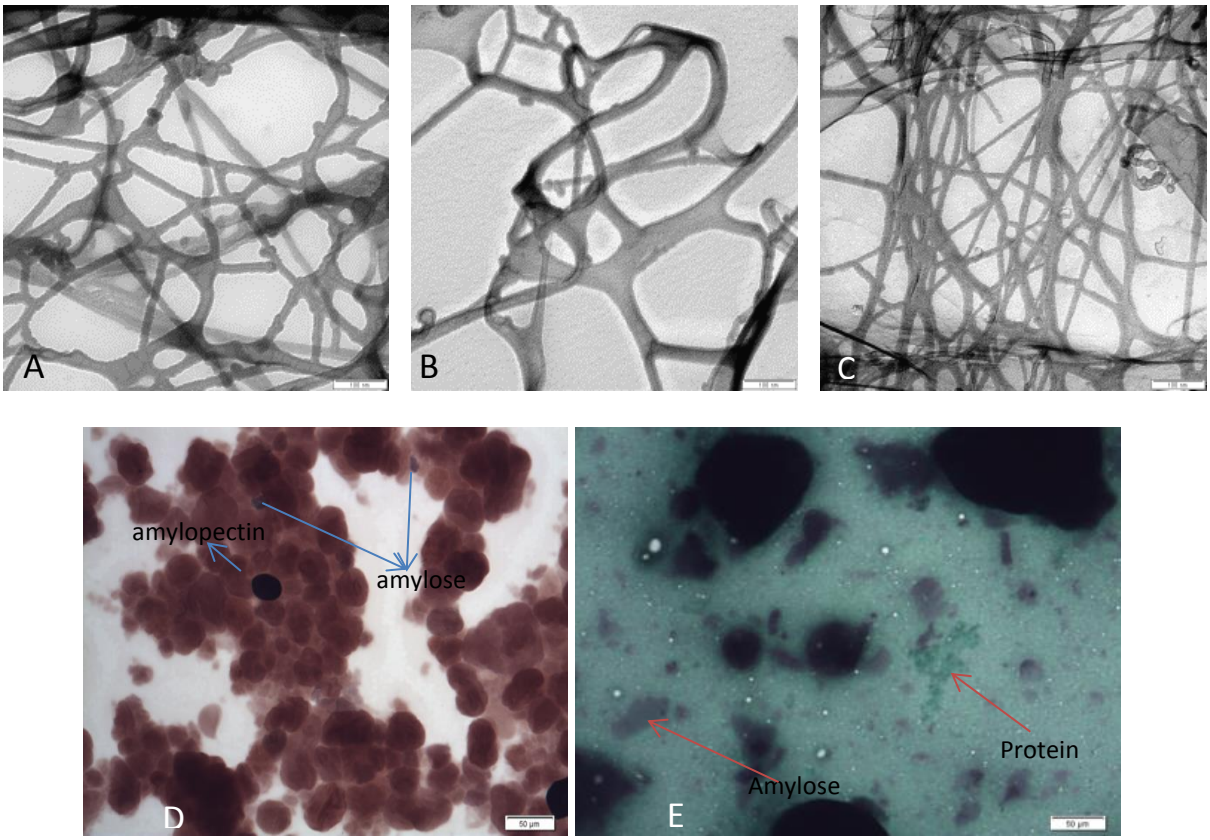

Figure 18: TEM micrographs of the xanthan gum-based thickeners: Fresubin Clear (A), Nestlé Clear (B), and Nutilis (C), and LM images of the thickeners: Nestlé Thicken-up (D) and Findus thickener (E). Note that the scale bars in panels A, B and C is 50 nm, and those in panels D and E are 50 µm.

For the starch based-thickeners, LM was the preferred technique due to the large structure of the starch granules (typically in the micrometre range). In the sample of Nestlé Thicken-up, swollen starch granules were detected. These swollen starch granules were light-brown in colour, indicating the presence of amylopectin (the principal component of a starch structure). In addition, there were some purple-stained starch granules, suggesting that an amylose fraction had leached out (indicated by arrows in Fig. 18 D). The remaining starch-based thickener, Findus thickener (Fig. 18 E), contains fats and proteins, in addition to starch. The proteins were stained green, while the fats were unstained in the sample. In the present study, the gum-based thickeners were found to have a low yield stress due to characteristic fine network structure on the nanometre scale, as seen with the TEM technique.
In the case of the starch-based thickeners, the principal structure was the swollen starch granules on the micrometre scale, as visualised in the LM study.

The reason for measuring the T_y here was mainly to assess which of the two categories of thickeners (starch-based or gum-based) possess T_y. The T_y values reported here are too low and therefore unlikely to influence the overall swallowing process, given that the bolus is never static during the oral and pharyngeal stages and is subject to stresses that are much higher than those indicated by the T_y values calculated here.

5. *IN VIVO* APPROACH TO STUDY DEGLUTITION

This section investigates the role of rheology (or more precisely, fluid elasticity) in safe swallowing. During bolus transport in the pharyngeal phase, the bolus is subject not only to shear but also to extension deformation, as it is squeezed between the tongue and the palate (Adam S Burbidge, 2016). modification of shear viscosity is known to confer beneficial effects, on the contrary it extensional rheology has not been studied well enough for its beneficial effects; to our knowledge, this study is the first to examine the impact of bolus elasticity on safe swallowing. This study involved actual patients, so it is of high relevance in the context of this thesis. This section provides an overview of the model fluids used in the clinical study, their rheological characteristics, and how model fluids with elastic properties affect patients who have a malfunctioning mechanism for swallowing.

5.1 Model fluids

Model fluids, which are fluids of known composition, are used here as a reference to distinguish pure elastic effects from pure viscous effects. In the current project, three model fluids (Newtonian, Boger, and shear-thinning) were created. These model fluids were used in the sensory analysis and in the clinical studies (**Paper I**).

Newtonian fluids

In **Paper I**, a model Newtonian fluid was constructed from maltodextrin. Maltodextrin forms a Newtonian solution and is not as sweet as syrup, so it could be used in the sensory study.

Boger fluids

Boger fluids (named after David Boger who introduced them in 1977) are fluids that have a constant shear viscosity, i.e., one that is independent of the shear rate. The main differences between Newtonian and Boger fluids is that Boger fluids are highly elastic at room temperature. Moreover, Boger fluids have a relaxation time that is similar to that of a molten polymer. Boger fluids are prepared by dissolving a very small amount of non-Newtonian fluid, typically of high molecular weight, in a viscous Newtonian solvent. The viscosity of the solvent masks the shear-thinning effects while maintaining the long relaxation time. A Boger fluid can be used to separate the pure elastic effects from the pure viscous effects, as compared to its Newtonian counter-part fluid. The Boger fluid used in **Paper I** comprised a maltodextrin solution as the Newtonian solvent and xanthan gum as the elasticity agent and a food-grade polymer.

Shear-thinning fluids

In **Paper I**, the edible shear-thinning fluids comprised maltodextrin and a higher concentration of xanthan gum. Thus, shear-thinning fluids are in practice more elastic than the Boger fluids, which means that they are likely to confer even better swallowing effects in patients.

5.2 Rheology of model fluids

The steady-state flow curves of the model fluids that were used in the clinical examination are presented in Figure 19. The model fluids (**Paper I**) needed to be radio-opaque, so as to allow video fluoroscopic visualisation. This meant that contrast media (barium- or iodine-based) had to be added to the model fluids. As barium-based contrast media are non-water-soluble, they were not suitable for use in the current study. Therefore, water-soluble iodinated contrast media were used in the model fluids for video fluoroscopy.

Xanthan gum, which to our knowledge is the most suitable elasticity-providing, food-grade polymer, was used to allow the model fluids to be used in the clinical experiments. The shear-thinning and Newtonian model fluids showed the expected behaviours of shear rate dependence (n=0.64) and shear rate independence (n=0.98), respectively. The Boger fluid showed a low level of shear thinning (n=0.87) at low shear rates due to the use of the contrast media. Nevertheless, its behavior is Newtonian, i.e., the flow curves converge with the Newtonian counter-part at shear rates ≥50 s^{-1}, which are the shear rates that are likely to occur during the swallowing process.

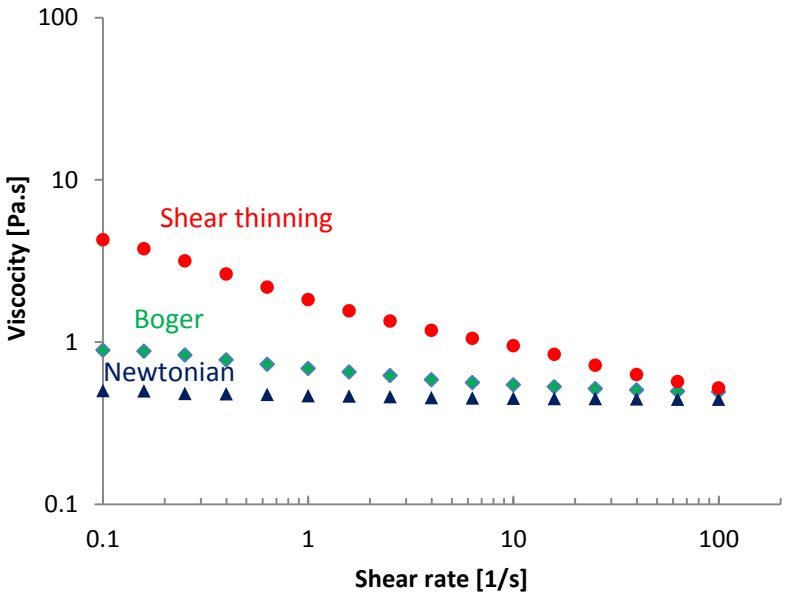

Figure 19: Flow curves of the following iodinated model fluids: shear-thinning fluid containing 500 ppm xanthan gum; Boger fluid with 200 ppm xanthan gum; and the non-elastic Newtonian counter-part (without xanthan gum).

To demonstrate that the iodine-containing model fluids were sufficiently elastic to confer health benefits, they were characterised in extensional deformation using the HCF technique (as mentioned earlier). The shear-thinning (iodinated) sample had an extensional viscosity in the range of 103–310 Pa.s when the extension rate was varied between 8 s^{-1} and 57 s^{-1} (Fig. 20), while the extensional viscosity of the iodinated Boger fluid varied in the range of 6.5–8.0 Pa.s (in the extension rate range of 13–27 s^{-1}). This indicated a substantial disparity between the two model fluids, even though the difference in the used concentrations of the elasticity-providing polymer, xanthan gum, was relatively small (500 ppm and 200 ppm). The disparity is attributed to an increased shear contribution in the hyperbolic nozzle as the Power-law flow index n approaches 1, resulting in a lower estimated

extensional viscosity. Thus, Power-law assumptions may not be appropriate for these types of model fluids.

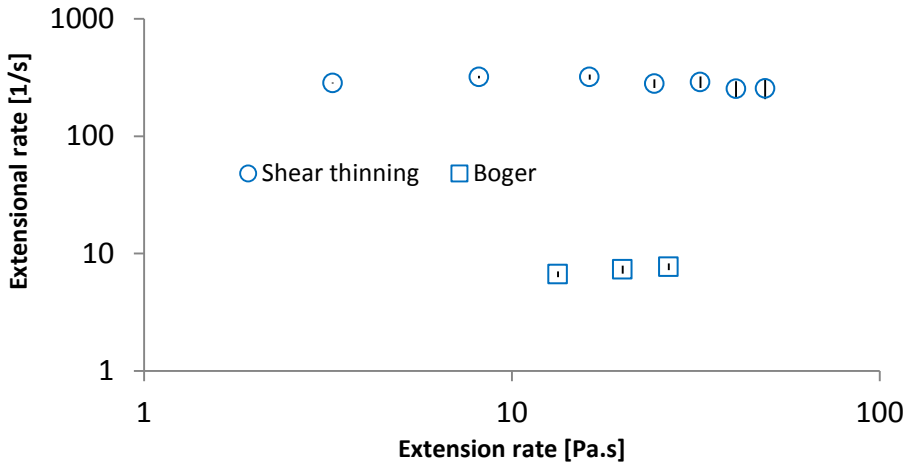

Figure 20: Apparent extensional viscosities of the iodine-based model fluids used in the clinical examinations. Shown are the results for: the shear-thinning fluid (500 ppm xanthan gum) (squares); and Boger fluid (200 ppm xanthan gum) (open circles). The lines inside the symbols represent the standard deviation

The main aim here was to demonstrate that the model fluids that contain xanthan gum are more elastic than the non-elastic Newtonian counter-part, and are therefore likely to exert effects in clinical studies. To validate the HCF results, a CaBER analysis was performed on the Boger and Newtonian fluids that were used in the clinical study (applying the experimental parameters listed in Table 3).

Table 3: Experimental parameters in the CaBER experiments

Model fluid	h_o	h_f	Hencky strain (1/s)	Surface tension (mN/m)	T (°C)
Newtonian	3	8.4	1.336	70.5	22
Boger	2	8.4	1.43	71.5	22

The diameter of the two piston was 1.2mm, h_0 and h_f referring to the initial height and final height, respectively,

In Figure 21, the filament-normalised diameters of the model fluids (averages of several measurements) reveal a longer capillary break-up time for the Boger fluid when compared to its Newtonian counter-part. The extensional viscosity calculated by CaBER was ~9 Pa.s (ε=6.4 s^{-1}) and 1.93 Pa.s (5.4s^{-1}) for the Boger and Newtonian fluids respectively.

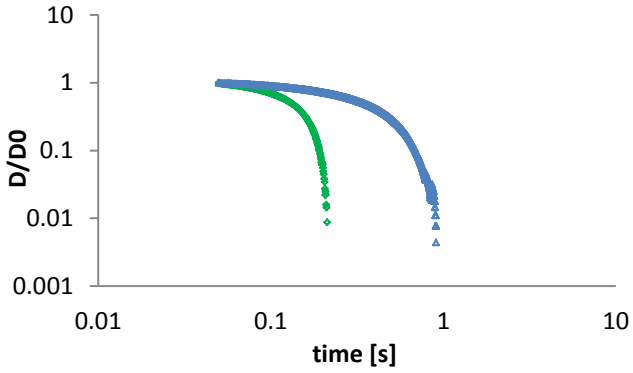

Figure 21: Filament-normalised diameter evolution of the model fluids over time at 25°C. The Newtonian sample (composed of maltodextrin) is shown in green, and the Boger fluid (60% maltodextrin and 0.02% xanthan gum) is shown in blue.

Unfortunately, the iodine-based shear-thinning fluid was not measured in CaBER. However, the first normal stress difference (N_1), which is also an indicator of the elastic behaviour of a fluid, was followed during the shear viscosity measurement, as reported in **Paper I**. The value of N_1 increased with increasing shear rate, and the increase was more pronounced in the shear-thinning fluid than in the Boger fluid. In this study, the shear-thinning fluid was more elastic (500 ppm), i.e., contained a higher concentration of xanthan gum than the Boger fluid (200 ppm). Increasing the shear rate did not affect the value of N_1 for the Newtonian fluid, indicating that the Newtonian fluid lacked elasticity, as expected. The Trouton ratios for the shear-thinning fluid and Boger fluid were 168 and 5, respectively, i.e., higher than the Newtonian limit of 3, which means that a reasonable experimental elastic contribution was detected in the model elastic fluids.

5.3 Sensory evaluations performed for healthy subject and for patients

A thorough sensory analysis was performed on the model fluids by a trained panel, to identify sensory attributes with respect to oropharyngeal bolus handling. Details of the sensory procedure applied by the trained panel and the panel of patients are given in **Paper I**. The results acquired by the sensory panel (Fig. 22 A) and the panel of patients (Fig. 22 B) are presented below.

During the sensory testing of the healthy subjects, shear-thinning effects appeared to predominate.

The healthy panel could not distinguish the elastic model fluids with respect to ease of swallowing due to the swallowing process being involuntary. Overall, mouth-feel attributes predominated over swallowing attributes in the healthy subjects. This was evidenced by the “thickness” attribute scoring the highest for the shear-thinning model fluid, which might be due to the low shear rates in the sensory tasting conducted by the health panel.

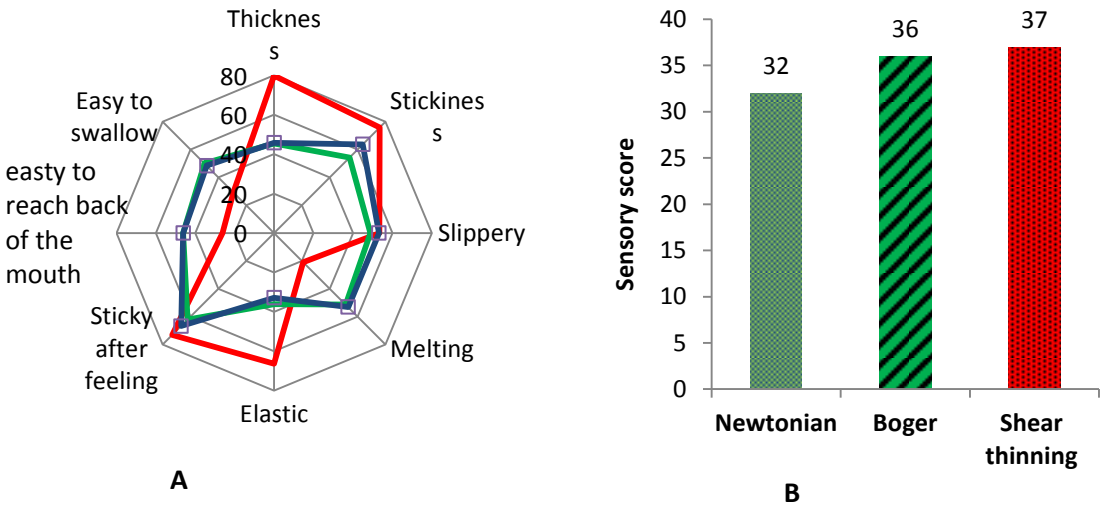

Figure 22: A) Spider plot showing 'mouth feel' and 'ease of swallowing' for the model fluids (Newtonian, blue line; Boger, green line; and shear-thinning, red line). B) Ease of swallowing responses of patients who have a swallowing disorder, represented as the total score on a scale of 1–5, where 1 is 'very difficult to swallow' and 5 is 'very easy to swallow'.

In contrast, the patients with dysphagia scored elastic fluids as being 'slightly easy to swallow' (Fig. 22 B). Thus, the highest scores for ease of swallowing were recorded for the elastic shear-thinning and Boger fluids (scores of 37 and 35, respectively), as compared to the Newtonian fluid (score of 32). This is understandable, given that these patients are more susceptible to misdirected bolus flow and are therefore more aware when swallowing fluids with different consistencies. However, as only twelve patients participated in the clinical study, the results obtained are not statistically significant (P>0.05). In addition, quantitative video fluoroscopy was performed, to assess further the effect of elasticity on safe swallowing. Fluids with elastic properties, the Boger and shear-thinning fluids were relatively easy to swallow.

5.4 Quantitative video fluoroscopy

The results for the patients with dysfunctional swallowing, quantified as Oral Transit Time (OTT) and Pharyngeal Transit Time (PTT), are presented in Figure 23.

There is some debate as to whether a fluid that transits faster during oropharyngeal swallowing promotes safe swallowing or has the opposite effect. The literature associates faster transit times with safe swallowing (Bulow 2003) (J. Chen *et al.*, 2011), probably because the liquid is recognized as being safe to swallow by the sensory receptor responses of the patients. In our tests, the average OTT was shortest for the elastic Boger fluid (indicating better swallowing) and longest for the non-elastic Newtonian fluid. The more important parameter of PTT was also shorter for two elastic fluids, the Boger and shear-thinning fluids (1.43 and 1.41 seconds, respectively) than for the Newtonian fluid (1.62 seconds). The PTTs recorded here are still much longer than those observed in clinical examinations with liquid foods (0.22±0.09 seconds) (Cassiani *et al.*, 2011).

As the study was performed with twelve patients, individual patients might show results that are different from the overall picture, as seen in the Figures. Regarding the influences of the model fluids on individual patients, five patients had the shortest PTT with the shear-thinning fluid and four of them had a short PTT with the Boger fluid. Only three patients had a shorter PTT with the non-elastic

Newtonian fluid. This indicates that fluids with elastic properties, regardless of the amount, are relatively easy to swallow.

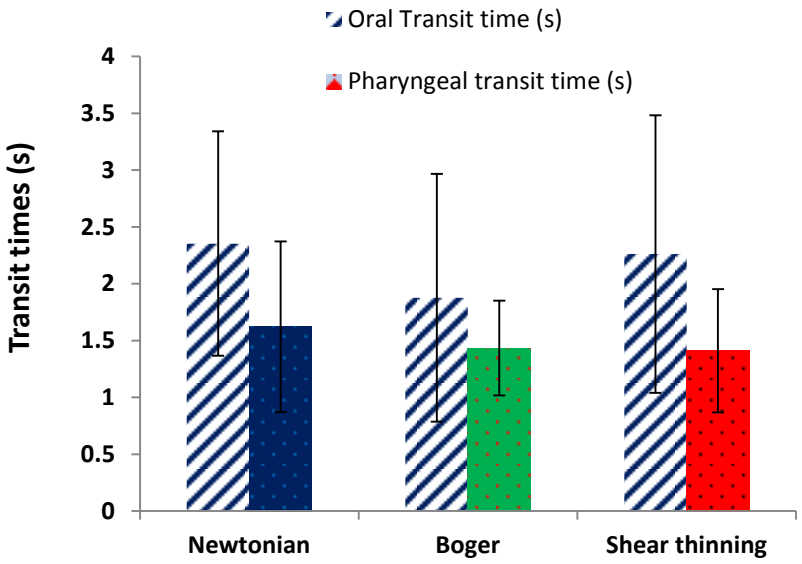

Figure 23: Average Oral and Pharyngeal Transit Times (in seconds) for the different fluids applied to the patients with dysphagia in the clinical study.

Note that the shear-thinning fluid, in this case, is even more elastic, since it only differs from the Boger fluid in that it has a higher concentration of xanthan gum (500 ppm). The observed differences were not statistically significant (P>0.05), highlighting the difficulties associated with testing the new hypothesis. The depth of penetration of the fluids into the airways and retention of contrast media in the pyriform sinuses were also studied. Both parameters are markers of misdirected swallow and bolus entry into the airways (**Paper I**). Three patients suffered aspiration into the sub-epiglottic region (mild aspiration). This was noticed for all the model fluids. Similarly, four out of twelve patients experienced mild pharyngeal retention, while one of the patients experienced severe pharyngeal retention with all the model fluids (Fig. 24).

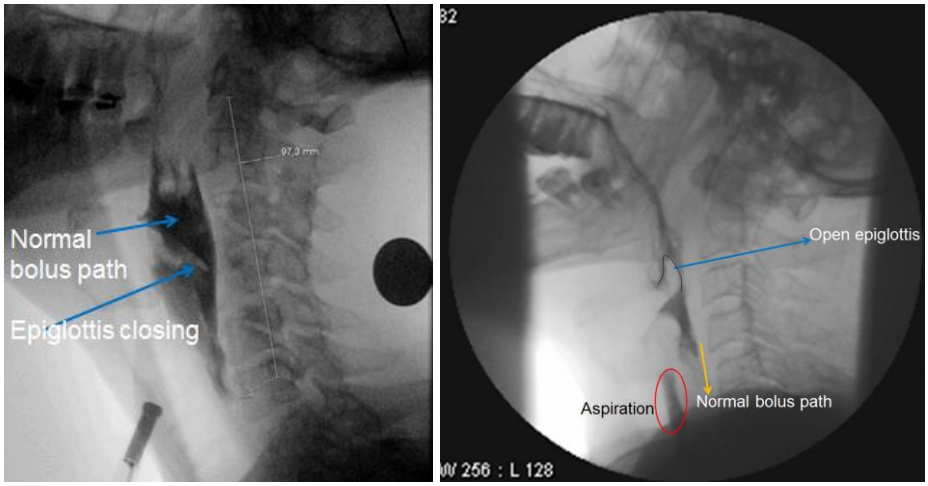

Figure 24: An example of normal swallowing in a healthy individual when a bolus is located in the pharynx while the epiglottis is closing (left panel), and an example of severe dysphagia (right panel), in which the model fluid enters the airways while the epiglottis remains open during bolus movement.
Note: In the example of normal swallow (left panel), a bolus volume of 15 ml and in the example of abnormal swallow (right panel) a bolus volume of only 5 ml was used.

Pharyngeal retention is an indication of weak pharyngeal muscles, which may lead to the appearance of residues from the swallowed food, as noted in some of the patients here. Overall, even though the fluids with elastic properties had positive effects, these effects were not apparent in some patients who were very severely affected by dysphagia. Various problems were experienced during the clinical studies including: the recruitment of a sufficient number of patients; categorisation of the patients into sub-groups; the use of contrast media, patient discomfort; and ethical issues.

These challenges made it very difficult to test the novel hypothesis that might confer beneficial effects as suggested in the recently published White Paper by the ESSD. For example safe swallowing in dysphagia promoted by fluid elasticity and the fluid yield stress or the shear rate range during swallowing. The alternative approach is to perform computational studies. However, the complexity of the human swallowing process makes this very difficult, and many assumptions have to be made during such studies, as discussed in detail elsewhere (Qazi & Stading, 2017). This provides the motivation for performing swallowing studies with respect to bolus rheology in an *in vitro* swallowing model that provides balances the two extremities of simulations and medical tests. In the following sections, we present the *in vitro* swallowing model, termed *The Gothenburg Throat*, as a pre-clinical study tool to study the linkages between bolus rheology and safe swallowing.

6. DEVELOPMENT OF THE *IN VITRO* DEVICE

The previous sections gave an overview of the rheology of thickened fluids. This was followed by a clinical study, which looked at the effects of fluid rheology on healthy individuals and on patients suffering from dysphagia. During the clinical study, a number of issues arose, which have been discussed earlier. The following sections describe in detail the construction and validation of the *in vitro* swallowing simulator, together with a discussion of the results acquired with the device.

Taking into account some of the shortcomings of the previous *in vitro* models mentioned in the book chapter (Qazi & Stading, 2017) , the *Gothenburg throat* was designed based on the following considerations:

- A geometry similar to the human pharynx in distended form, with dimensions taken from the literature;
- Simulation of the physiological processes that occur during swallowing, i.e., the closing of the vocal chords and the upper oesophageal sphincter (UES), opening and closing of the epiglottis, and opening to the nasopharyngeal channel;
- Monitoring of the bolus velocity profile during swallowing;
- Pressure measurements at different locations of interest, i.e., at the entrance to the pharynx, at the entrance to the trachea, mid-pharynx before the UES, and in the nasopharynx;
- A transparent pharyngeal channel for visual observations; and
- A temperature control system

An overview of the *in vitro* model is shown in Figure 25, and the individual components are described in detail below.

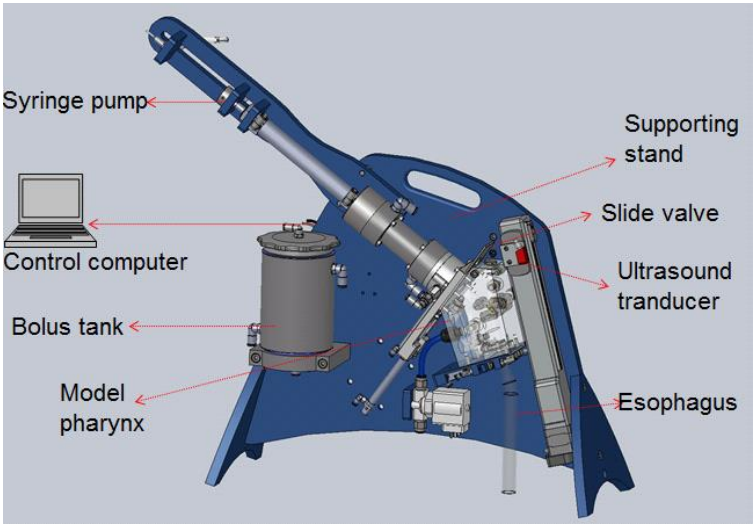

Figure 25: Schematic of the model in-vitro swallowing simulator showing the different parts.

6.1 Model pharynx material properties, components, software, and temperature control system

The material chosen for the device was Accura® ClearVue, which is a commercially available polycarbonate-like, 3D-printable, plastic material from 3D Systems (Rock Hill, South Carolina, USA). The model Pharynx was 3D-printed from a 3D drawing, which was based on geometrical specifications taken from the literature.

The material was chosen owing to its suitability for usage in medical models, its transparency (allowing fluid flow visualisation), and its resistance to liquids. This material is also suitable for 3D printing. Additional, smaller components used to construct the device are listed in Table 1 of **Paper III**.

The software used to control the device regulates various components, such as the tank holding the fluid, the syringe, valves, lids, and movement of the ultrasound transducer.

The interval between bolus injections can be set in seconds. Measurements can be stopped at any time during bolus flow. Opening and closing of the structures (epiglottis, glottis, nasopharynx, UES, and slide valve) can be timed to reflect different physiological conditions. The software executes all the necessary control functions, including: 1) regulation of the motions of the structures of the nasopharynx, trachea, and UES; 2) control of the valves for the trachea and nasopharynx; and 3) control of the pneumatic operation of the syringe and slide valve responsible for injection of the bolus. Between batches, cleaning is performed by attaching the bolus tank to a source of tap-water, and flushing with water at a constant flow that is regulated by the software.

To mimic accurately body temperature, channels are installed that circulate temperature-controlled warm water from a water bath around the model pharynx and into the syringe that delivers the bolus (Section 6.4; Fig. 27). The propelling of the syringe can be regulated by either force or a speed-based control system.

6.2 Simulation of bolus injection

The operation of the model starts with bolus injection, assuming that the bolus is already prepared. A syringe pump delivers a bolus of defined volume (5–30 ml) with a defined speed (~0.5–1.0 ms^{-1}) to the pharynx, which is equivalent to the thrusting action of the tongue. The bolus is loaded from a tank, enabling automated, repetitive measurements. A sliding valve is located after the syringe, before the entrance to the pharynx, to prevent gravity-induced flow before active bolus delivery.

6.3 Dimensions of the model pharynx

The dimensions of the model pharynx were taken mostly from the literature, while minor adjustments were made to accommodate the functioning of the mechanical parts. Thus, the pharynx in the model is elliptical in shape (Fig. 26), with a length of 6.3 cm, as described in a previous study (Walsh *et al.*, 2008), and a width of 2.8–3.0 cm at its widest point (Salinas-Vázquez *et al.*, 2014). The entrance to the pharynx has a circular area of 314 mm^2 (diameter of 20 mm). The circular entrance area is a compromise solution so that a syringe pump with a circular cross-section can be used for bolus delivery. The epiglottis in the model has a length of approximately 11.3 mm, maximum diameter of 12.5 mm, and average thickness of 1.87 mm (Kano *et al.*, 2005).

The junction between pharynx and esophagus in the current model is 4.3 cm in length with an elliptical entrance (area of196 mm^2), as described in literature (Morinière *et al.*, 2013). The

esophageal structure is modelled by a transparent rubber tube that is 20 cm in length and 1.7 cm in diameter, mimicking the human physiology (W. J. Dodds, 1989). The nasal cavity has a circular cross-sectional area of 78 mm² (diameter of 10 mm) and length of 40 mm. The model trachea is 57.13±7.32 mm in length, with a circular shape with diameter of 12 mm and internal diameter of 12.3 mm (Joshi *et al.*, 2011).

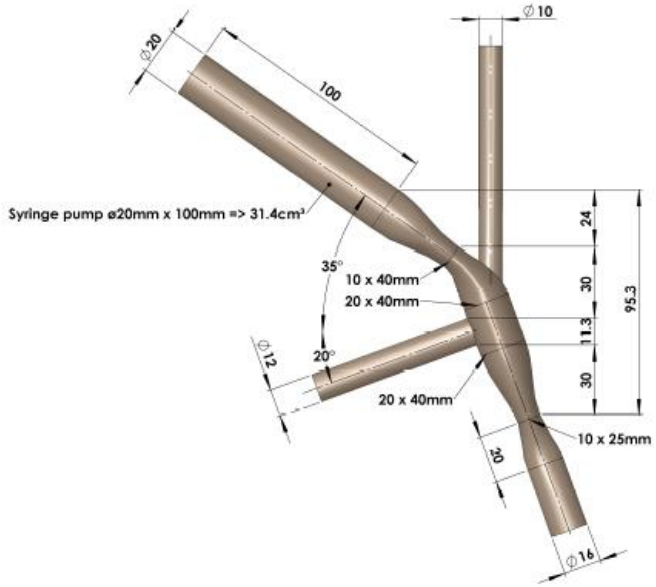

Figure 26: Dimensional specifications of the model pharynx and adjacent structures.

6.4 Simulation of the different entrances and exits to and from the model pharynx

As mentioned in the previous section, the bolus is injected into the model pharynx using a syringe pump. There are three exits from the pharynx, resembling the biological counter-part. These exits are located at the nasal cavity, larynx, and UES, as the bolus is transferred towards the oesophagus. The exit at the nasal cavity can be opened and closed by a valve (Fig. 27), while a revolving lid controlled by a motor that can open and close provides further control for air release. Actual swallowing is followed by expiration and the released air contains flavour compounds, which are transported to the nasal cavity to provide the characteristic flavour of a given food. At the exit of the nasal cavity, a connection that is attachable to a Tenax® tube is made to enable capture of the released air, thereby allowing flavour chemistry studies. The second exit in the model pharynx is towards the model trachea, which although it is static in the model as opposed to dynamic in actual swallowing is protected from bolus leakage by the epiglottis and a solenoid valve that prevents air-flow through the trachea. The third exit is the esophageal exit, which is also the normal path that a bolus takes when transported towards the stomach. The bolus has to pass through the all-important UES junction before entering the esophagus. The UES, which is normally in a closed position, thereby protecting the airways from any reflux of stomach contents, opens momentarily (for 415±66 ms) (Morinière *et al.*, 2013) to allow passage of the bolus. The model UES junction is regulated using a pneumatic pinch valve that can be timed for periods up to milliseconds and for several repetitions in the case of multiple bolus injections.

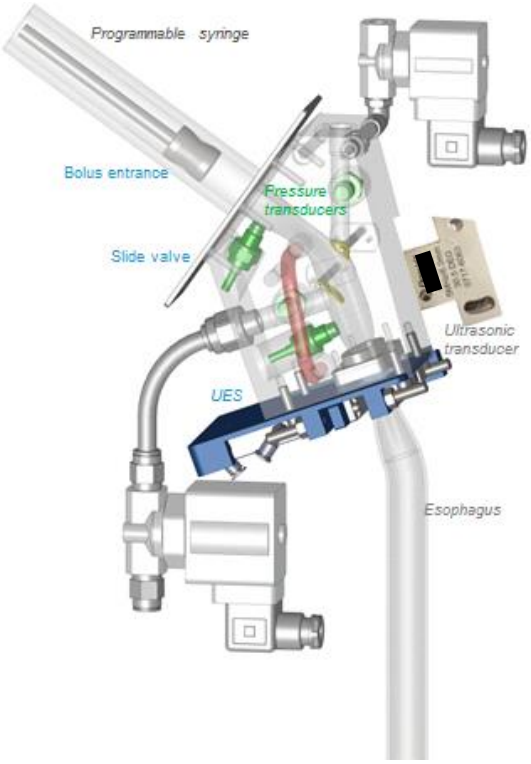

Figure 27: Schematic of the modelled epiglottis (yellow), nasal cavity, upper esophageal sphincter (circled), opening/closing function of the UES controlled by a clamp valve (blue), pressure transducers (green), the warm water channel (red), and the part of the trachea that recovers the leaked fluid when abnormal swallowing is simulated.

6.5 Pressure and UVP measurements in the model

The present project was designed to perform *in vitro* measurements of the *in vivo* counter-part, invasively in the developed swallowing device. This capability is not featured in any of the previous *in vitro* devices/simulations. A detailed discussion of *in vitro* swallowing studies is provided in the book chapter (Qazi & Stading, 2017). The analysis of *in vivo* swallowing is performed using two techniques, manometry and video fluoroscopy, whereby the latter allows the examiner to follow the sequence of events occurring during pharyngeal bolus transport. In the present work, apart from the performance of manometry using a pressure sensor embedded in the model pharynx wall, bolus velocimetry was performed using the UVP technique, which traces bolus movement non-invasively. The results presented in **Papers, III and IV** are based on measurements taken with the UVP technique. To detect and present physical activities, including bolus transport and the pressure applied, a transducer system was designed and installed in the model pharynx, as shown in Figure 27. A brief description of these pressure transducers is presented in the following sections.

6.5.1 Pressure transducers

Pressure transducers from TE Connectivity (Paris, France) were installed in the model at four locations: the pharyngeal entrance; the mid-pharynx; near the UES; and the nasal cavity (Fig. 27). The pressure transducer can measure in the range of 1±48 kPa with the given electronic settings, which is sufficient to mimic most of the pressure values reported during human swallowing, which are typically around 48 kPa for men and 42 kPa for women (Alsanei *et al.*, 2014).

6.5.2 Pressure measurements during continuous and bolus flows

Pressure measurements were performed using pressure transducers and an oscilloscope with monitoring software from Pico Technology. The linear range of the voltage that corresponds to the pressure (kPa) as an output is defined in the Pico Scope 6 software. To measure the dynamic pressure applied by the bolus, the electronics are set to filter out the static pressure using a high-pass filter. However, the high-pass filter is not installed on the transducer that is installed on the nasal cavity. This transducer acts as a control, as it does not come in direct contact with the bolus. The pressure recorded at this location is subtracted from the acquired values, to calculate the final pressure values as the corrected pressure in the model pharynx, as is done in **Papers III and IV**.

A T-connection (Fig. 28) was built such that the pressure transducer in the mid-pharynx was connected on one end, and a calibrated digital reference pressure transducer, DPI 705 (Amtele Engineering AB, Stockholm Sweden), was connected on the other end. Compressed air was introduced into the T-connection. The pressure output (on the digital screen) from the reference transducer was compared with the pressure values displayed in the Pico Scope software from the model pharynx transducer. The compressed air flow was gradually increased from 1 kPa to 48 kPa, to cover the entire range of pressures that is measurable inside the model pharynx. The method was repeated several times to ensure repeatability.

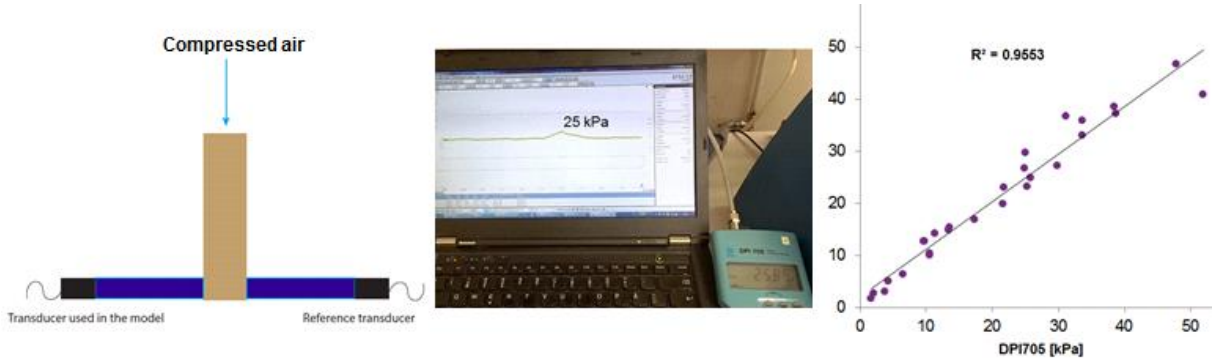

Figure 28: Calibration of pressure transducers against the reference pressure transducer DPI 705. Schematic of the T-connection (left panel), demonstrating the result on a PC with the reference transducer (middle panel), and the overall calibration curve for the reference and the pressure transducer used in the model (right panel).

A difference of only <6% was noted when applying a least-squares regression line, i.e., R^2=0.955. Since all the transducers are designed in the same way, it is assumed that every transducer installed in the model pharynx will provide an output of similar accuracy. The results obtained from the *in vitro* manometry are presented in **Papers III** and **IV**.

6.6 UVP measurement in continuous fluid and bolus flows inside the model pharynx

Flow visualisation was performed using the Ultrasound Velocity Profiling (UVP) technique with a commercial UVP system that includes the electronics, software, and US transducers (Incipientus™; Ultrasound Flow Technologies AB, Gothenburg, Sweden).

6.6.1 Experimental loops used to measure continuous fluid flows

To measure the rheological characteristics of the thickeners used in dysphagia management (**Paper II**), and to validate the velocity profiling in an elliptical geometry, two different flow loops were constructed. The flow loop described in detail in **Paper II** was based on two transducers of frequency 8 MHz, installed at an angle of 20º on a stainless steel pipe with length of 0.6 m and radius of 0.011 m. The flow loop used in **Paper III** is shown in Figure 29 and is described briefly below.

The fluids were continuously pumped in the model throat from a tank using a rotatory lobe pump. The pump was operated at two different speeds, corresponding to two flow rates expressed in litres/min in this study (**Paper III**). While pumping proceeded, the entire model was filled with the fluid and the valves on the larynx and nasal cavity were closed prior to performing the measurements, to avoid the escape of the liquid into these cavities. Thus, the liquid flowed continuously in a loop from the model pharynx to the tank through a pipe.

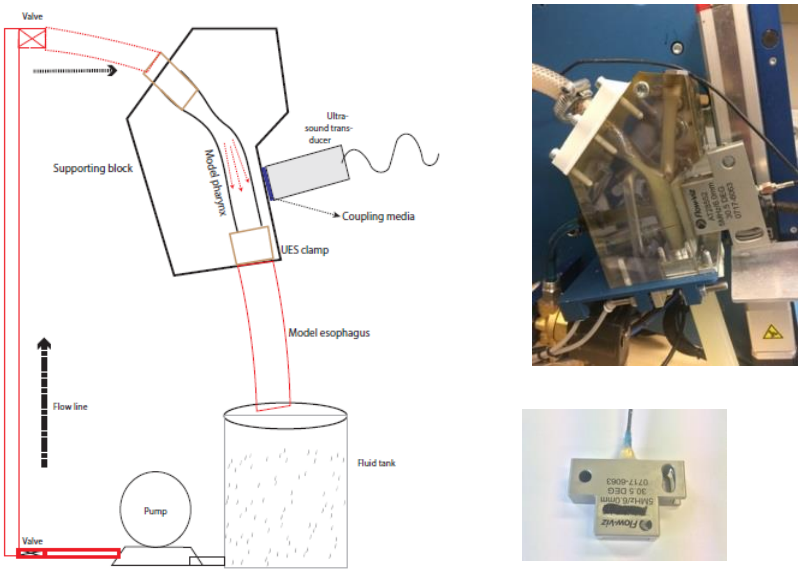

Figure 29: The flow loop used to measure the velocity profiles and manometery during continuous pumping of fluids. The left panel shows a schematic of the measurement set-up. The upper-right panel is an image of the actual measurement set-up, while the lower-right panel is an image of the ultrasound transducer that was designed to measure the velocity profiles inside the model pharynx.

The ultrasound transducer, which was designed specifically for the *in vitro* swallowing model, is non-invasive; it was operated at a frequency of 5 MHz for five cycles per pulse.

To ensure firm contact between the transducer face and the model, the US transducer is attached to the model through a mechanical holder. To facilitate optimal transmission of the acoustic waves, appropriate acoustic coupling media were added between the transducer face and the model pharynx block. The temperature of the fluid was strictly followed - it varied between 20.5˚C and 22.0˚C during the measurements. The voltage and gain settings were varied depending on the fluids examined and the formation of any air bubbles during the flow.

6.6.2 Methodology for UVP measurements inside the model pharynx

A common problem encountered with 3D printing is that the dimensions may not be exactly the same as initially defined. In UVP measurements, precise knowledge of the location of the initial and final positions (channels) on the ultrasound beam axis within a cavity is of primary importance. The two positions are used to convert the measuring channels into radial positions, so as to integrate the velocity profile. This enables determination of the volumetric flow rate, which is needed as an input to calculate the final rheological parameters.

Therefore, the inner distances (a and b) inside the model pharynx were determined using an echo signal acquired from the inner wall of the given geometry and the conventional time-of-flight method:

$$s = \frac{ct}{2} \qquad [6.1]$$

where *s* represents the distance, *t* is the total time between the transmitted and received US pulse, and *c* represents the sound velocity. While sending the ultrasound beam the model pharynx cavity was filled with water, as the velocity of water is a known value. Based on the ultrasound analysis, the elliptical pharyngeal dimensions in the final model were 8.4 mm (short-axis) and 18.2 mm (long-axis), indicating a geometric variation of ~5%, which was taken into consideration when performing calculations on the acquired results.

Furthermore, in the measurement setup, the ultrasound beam passes through the polyamide material of the model pharynx into the actual fluid flow (Fig. 30). This means that the ultrasound beam is refracted inside the pharynx where the fluid flow is taking place. Therefore, the angle needs to be determined correctly, to ensure the accuracy of the velocity and shear rate measurements. The Doppler angle, i.e., the angle between the fluid flow and the ultrasound beam, was measured using a reference 90° ultrasound beam and the transducer designed for the model that operates at an angle. The two values were utilised to determine the angle inside the model pharynx for the test fluids.

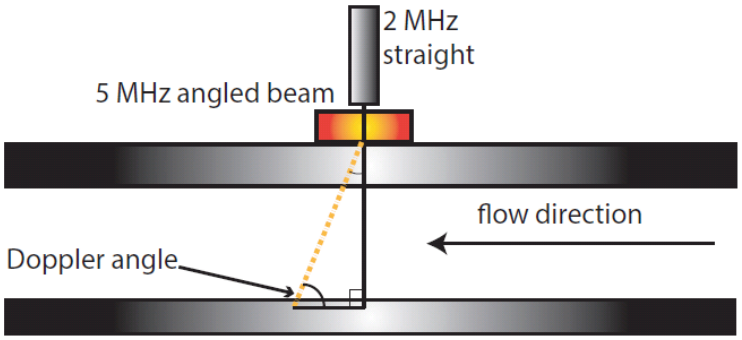

Figure 30: Schematic of the device for the measurement of the correct distance and angles for given fluids, inside the model pharynx. Two sensors with frequencies of 5 MHz and 2 MHz attached to the wall send the US pulses at an angle (broken yellow line) and in a straight line (black line), respectively.

Finally, the velocity of sound in the test fluids was measured off-line inside a stainless steel cell/block using the time-of-flight method. The sound velocity could be calculated by re-arranging Eq. [6.1]. On average, 64 velocity profiles were used to determine the volume flow rate and shear rate. A Doppler angle of 60˚ was determined, while the sound velocities in rapeseed and Fresubin Clear were 1443.6 m/s and 1560 m/s, respectively. The base frequency of the non-invasive ultrasound sensor was 5 MHz and five cycles per pulse were used for the velocity profile measurements. The voltage and gain settings varied depending on the fluid being tested and whether any air bubbles were present in the mixture.

7. EXPERIMENTAL VALIDATION OF THE *IN VITRO* MODEL

Various approaches were applied to validate the flow measurements inside the model pharyngeal cavity. These included running model fluids in continuous flow using externally connected pumps with different flow rate capacities, and running model Newtonian, shear-thinning fluids to evaluate the shapes of the acquired velocity profiles. The accuracy of the velocity measurements made inside the model pharynx were compared with gravimetric flow rate measurements (**Paper III**). To validate the velocity profiles using UVP and subsequent rheological measurements, the results acquired for different fluids (Newtonian, Power-law shear-thinning, and yield stress fluids) were compared with the results obtained using conventional rheometers. In addition, *in vitro* manometry was validated by applying a known external pressure and comparing the outcome with the results provided by the transducers installed in the model pharynx. Furthermore, the differences between the fluid pressures and atmospheric pressure with respect to flow rates were validated through comparison with theoretical pressure drops, e.g., according to the Hagen-Poiseuille law.

7.1 Validation of the UVP method by comparing with results from conventional rheometry

UVP+PD has been developed and demonstrated to measure the real-time rheologies of many industrial fluids (Wiklund *et al.*, 2007; Wiklund *et al.*, 2008). Industrial fluids are conventionally pumped in pipes of larger diameter, which are usually circular in shape. The UVP+PD technique was designed to measure the velocity profile during bolus flow and in the model pharynx, the size of which is smaller and more complex than many industrial pipes. Therefore as a starting point, a circular pipe of much smaller diameter (0.011 m) was used, as described in Figure 1 of **Paper II**. Thickeners were used in the study owing to their direct connections with dysphagia. The acquired results were compared with those acquired using conventional ARES-G2 (TA Instruments, Newcastle, DE, USA) measured under similar conditions of temperature (25ºC) and with almost identical range of shear rates. The resulting flow curves are presented in Figure 31, A and B, and the Power-law parameters in **Paper II**. The rheological behaviours of the fluids are discussed in **Paper II**. The focus here is on the goodness of the fit of the two methods for rheology measurements.

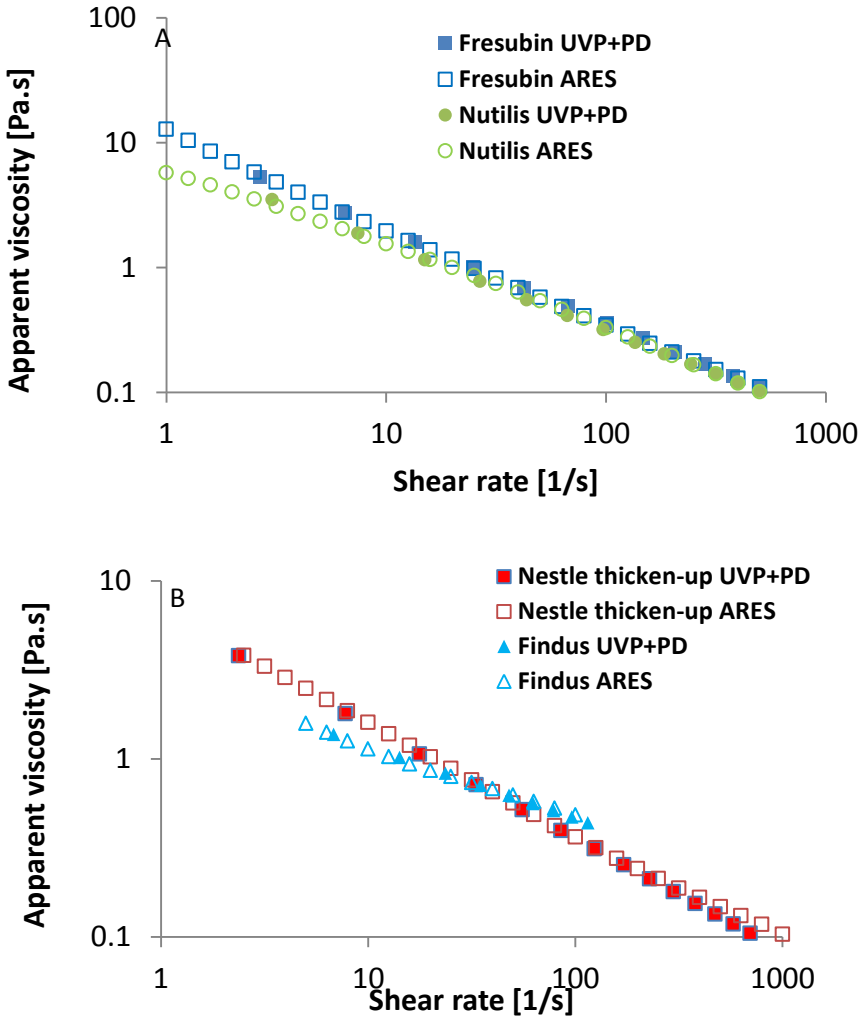

Figure 31. (A) Shear viscosities (Pa.s) of xanthan gum-based thickeners in water. (B) Shear viscosities (Pa.s) of starch-based thickeners in water.

The flow curves derived using the UVP+PD method overlapped almost perfectly with the flow curves acquired using laboratory-based rheometry. The two methods agreed very well (R^2>0.99) when comparisons were made at the same shear rates. Similarly, the comparison of Power-law parameters (**Paper II**) showed good agreement with a slight discrepancy in some samples, probably due to uneven mixing or the remnants of residues in the UVP+PD pipes/connections from samples of different consistencies measured in previous batch(es). Moreover, with the UVP+PD method, not many velocity points could be measured, especially in the low-shear-rate region, mainly due to the inherent inaccuracy of the manual control of the pump that regulates the flow rate.

Furthermore, the yield stress measurement, carried out with UVP+PD and compared with conventional rheometry (Section 4.3), is more reliable as there is no wall slippage. In the UVP+PD method, the yield stress is measured from the plug of the velocity profile in the middle of pipe and the pressure drop, as shown in Figure 17. This avoids direct contact with the geometrical walls. During conventional rheometry, wall slip is commonly encountered in geometries for rheological measurements, due to the presence of a wall. Wall slip results in displacement of the dispersed phase (which has higher viscosity) away from the wall, resulting in a depleted layer of low viscosity at the wall (Howard A Barnes, 1995).

7.2 Validation of bolus velocity using the UVP method in comparison with X-ray video fluoroscopy

The UVP method has been verified clinically against the standard method of swallowing examination, which is video fluoroscopy during bolus transport. A 15-ml bolus thickened to a consistency of 0.15 Pa.s (at 50 s^{-1}) using a commercial thickener mixed with water and an iodine-based contrast media was swallowed by a volunteer and examined simultaneously with video fluoroscopy and the UVP method. For this examination, a 4-MHz UVP transducer connected to the UVP measurement box was utilised (Fig. 32).

Two different types of velocities were compared: the maximum velocity, which is the distance travelled by the bolus head; and the velocity of the contract wave. These velocities were estimated from the distance travelled and the frame rate in video fluoroscopy.

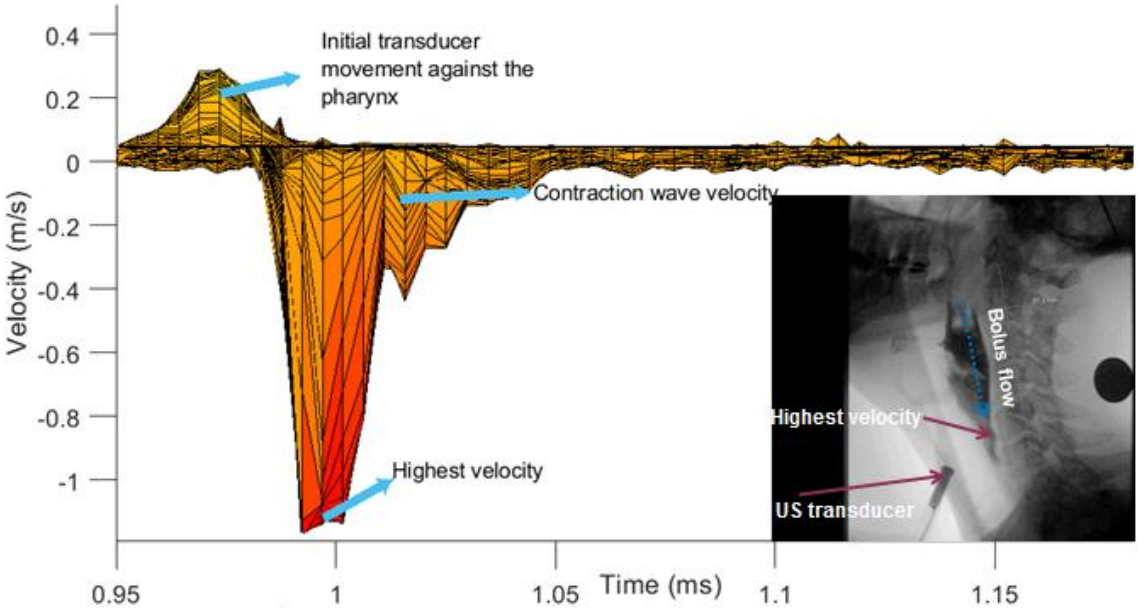

Figure 32: Velocity profile recorded during bolus transport using the UVP method and the corresponding image showing the bolus flow of the same swallow recorded with video fluoroscopy.

The highest velocities acquired from UVP and video fluoroscopy were 1.16 m/s and 0.87 m/s, respectively, yielding a variation of ~30%, which is quite reasonable considering that the UVP method has a much better time resolution of 47 ms than video fluoroscopy (62.5 ms) (videos were recorded at 16 FPS). Another interesting comparison of the two techniques was made for the velocity of the contraction wave that follows bolus transportation. Based on a previous report (Mashimo, 2006), this contraction wave is much more consistent and is independent of the bolus properties. The velocities of the contraction waves measured using the UVP method and video fluoroscopy were 0.15 m/s and 0.18 m/s, respectively, revealing a difference of only ~18%. This comparison was consistent for fluids having different consistencies and tested on different subjects. Further details are provided in a separate paper that is not part of this thesis work (manuscript under preparation). The results obtained here indicate high sensitivity for the UVP method. Therefore, the UVP method is a valuable tool to perform velocimetry and subsequent rheological calculations during bolus transport, as discussed below.

7.3 Study of velocity profiles in continuous flow while pumping Newtonian and non-Newtonian fluids

Fluid flow in a pipe of circular geometry is manifested with a characteristic velocity profile, under laminar conditions. In the centre of the pipe, particles travel at high velocities, while the particles located at the wall of the pipe remain almost stationary. Measurement of velocity profiles in a geometry that is not entirely circular is not very common. In this section, the velocity profiles of model fluids in a circular geometry are presented. Thus, maltodextrin (Newtonian fluid), water (Newtonian), and ketchup (yield stress fluid) were pumped into the model pharynx geometry (Fig. 33A–C). The resulting velocity profile measured with the UVP technique for maltodextrin (Fig. 33 A) was parabolic, as expected in the case of Newtonian fluids with Power-law index (*n*) of 1.

Ketchup is generally considered as a yield stress fluid (Berta *et al.*, 2016). When pumped into the model pharynx, ketchup was expected to present a plug-shape velocity profile, as shown in Figure 33 B.

To examine the velocity profile of water under a turbulent flow regime, a low number of particles were seeded into water such that the viscosity was not overly affected. When the seeded water was pumped through the model pharynx, the recorded velocity profile (Fig. 33C) was much flatter due to the turbulent flow behaviour of water (Reynolds number >2,500). When a fluid flows through a pipe under a turbulent flow regime, such as the seeded water in this case, the velocity profile acquired is often flatter in the centre of the pipe, as was the case here. The resulted velocity profile is best expressed by the Power-law velocity profile as:

$$\frac{v}{v_{max}} = \left(1 - \frac{r}{R}\right)^{1/n} \qquad [7.1]$$

The exponent *n* is a constant whose value depends on the Reynolds number and is often equal to 7 for turbulent flow in most applications. The index, which generally predicts many turbulent flows, is also referred to as the 1/7th Power-law velocity profile (R.P. Singh *et al.*, 2009).

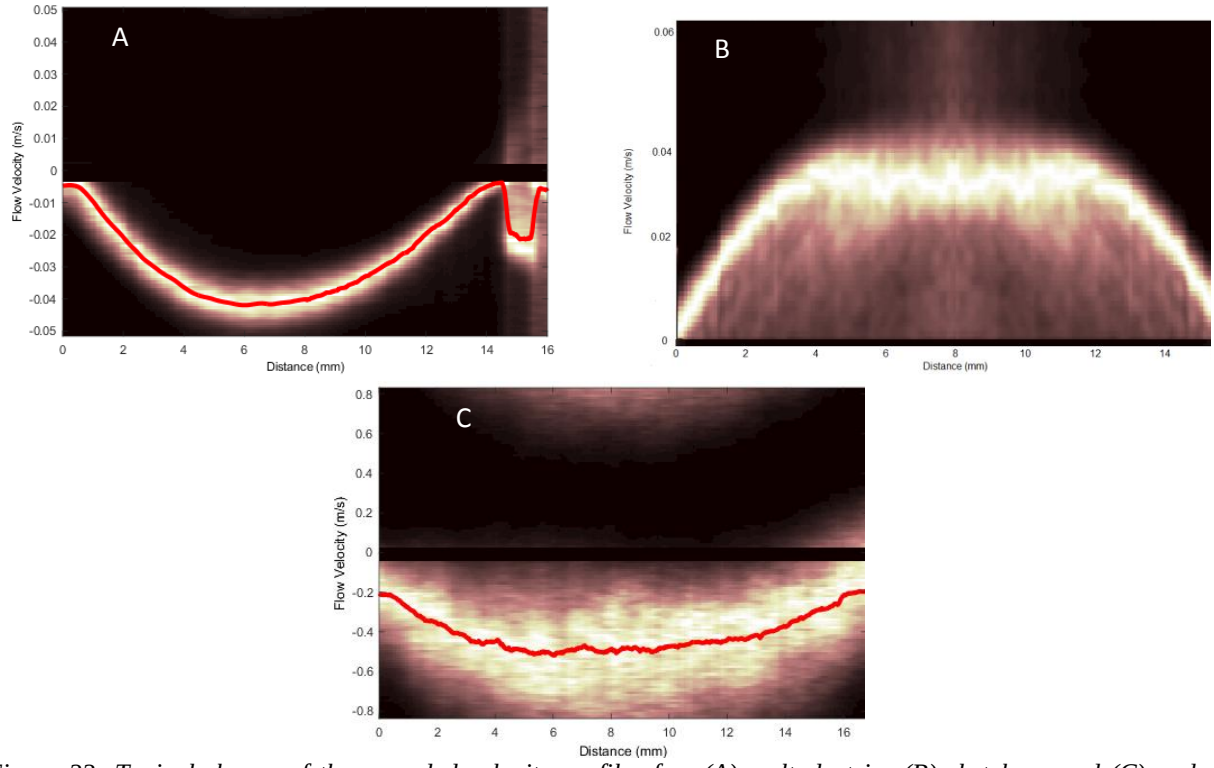

Figure 33: Typical shapes of the recorded velocity profiles for: (A) maltodextrin; (B) ketchup; and (C) and water seeded with particles. Negative velocities indicate fluid flows away from the ultrasound transducer.

7.4 Volume flow rate in elliptical geometry: theoretical considerations

The volumetric flow rate can be determined through integration of the velocity profile. This requires calculation of the total flow rate based on the correct velocity distribution inside the ellipse geometry. However, the literature regarding ultrasound velocity profiling in ellipses is scarce. Only one published article (John, 2007) has taken the Newtonian velocity profile into account.

L. Johan (John, 2007) described the total flow rate in an ellipse for a Newtonian flow using the flow/area distributions shown in Figure 34 and Eq. (7.2):

$$Q = \frac{\pi}{2} Vab \qquad (7.2)$$

where V is the maximum velocity in the ellipse, and a and b are the dimensions of a given ellipse, in this case 8.4 mm and 18.2 mm, respectively.

However, since a non-Newtonian fluid was used in the present work, the flow rate had to be determined using the measured velocity profile and numerical integration. The volumetric flow rate (Q) is calculated using Eq. (7.3):

$$Q = V.A \qquad (7.3)$$

where V is the velocity, and A is the total area of the geometry within which the flow is taking place.

To calculate a flow rate from the velocity profiles measured inside the ellipse geometry, separate flow rates were calculated for each area/flow segment and summed to yield the total volume flow rate:

$$Q = \sum_{n=1}^{N} (V_n A_n) \qquad (7.4)$$

where V_n is the measured velocity in the area segment A_n of the ellipse geometry of the pharynx model and N represents the number of segments.

The area of an ellipse is given by:

$$A = \pi ab \qquad (7.5)$$

where a is the shorter and b is the longer axis of the ellipse. Equation (7.5) was incorporated into Eq. (7.4) to determine the correct flow rate inside the ellipse.

Figure 34 shows the different area segments (A_n) used in the ellipse geometry, together with the actual dimensions (a and b) and the ultrasound sensor position (measuring line). Each area segment (A_n) has the same velocity distribution (obtained using UVP), and these were then summed to determine the total volume flow rate using Eqs. (7.3) and (7.4).

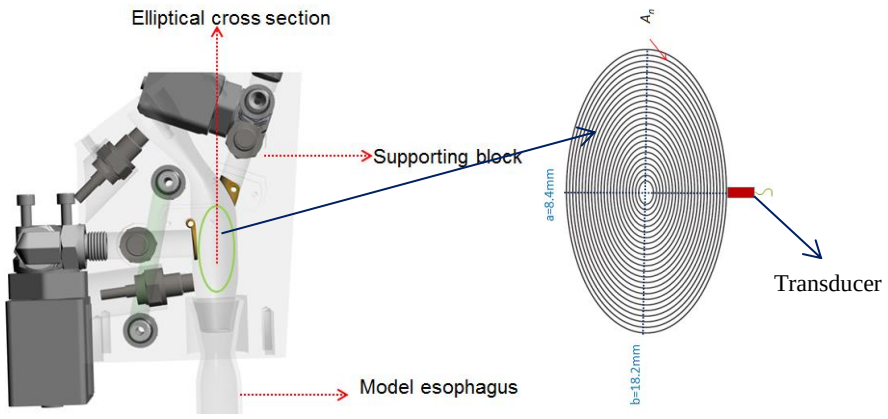

Figure 34: Schematic of the elliptical-shaped pharynx in the in vitro model (left) and the geometry showing the dimensions (a and b) and area distributions for the flow rate calculations (right). The velocity profile is measured across the short axis a, where the ultrasound sensor is positioned.

7.4.1 Verification of the flow in the elliptical channel using the gravimetric method (reference method)

The conventional gravimetric method was used as a reference to compare the flow rates and, thereby, validate the acquired velocity profiles in the model pharynx. Initially, the mass flow rate ($\dot{m}$), following the gravimetric method, was calculated, and this was then converted to the volumetric flow rate $\dot{Q}$. Direct measurement of ($\dot{m}$) has the advantage over volumetric flow rate that the mass is conserved during flow, whereas volumetric flow rate is subject to changes depending on physical properties such as pressure and temperature. Details of the gravimetric method, the results, and the comparison made with the integration of velocity profiles acquired with the UVP method are provided in **Paper III**.

7.5 Validation of pressure monitoring

The pressure validation set used to measure bolus thrust yielded reasonably good agreement (R^2=0.95), as discussed in Section 6.5.2. Validation was performed by applying a known pressure and measuring the elicited responses from the pressure transducers in the model pharynx. Slight variations were noticed in the upper region of the applied pressure. These were mainly attributed to the manually controlled applied pressure valve, the control of which was difficult at the upper limit of the pressure applied. Similarly, good agreement (<10% variation) was noted when Newtonian and shear-thinning fluids were pumped at two different flow rates and the resulting pressure drop was dimensionalised according to Hagen-Poiseuille law, as discussed in **Paper III**.

8. BOLUS FLOW IN THE "GOTHENBURG THROAT"

So far, our discussion has been mainly related to the *in vivo* analysis, the rheology of the fluids, and the construction and validation of the device. This section presents the results from the *in vitro* device with respect to bolus consistency, velocity, and shear rate. Moreover, the results obtained from *in vitro* manometry analyses (**Paper IV**) and how they are influenced by bolus consistency and volume at different locations in the model pharynx are discussed. The results are complemented with images acquired using the camera and the analysis of these images.

8.1 Velocity profiles of boluses thickened with a commercial thickener

Thickened boluses produced by major manufacturers, i.e., Nestlé Thicken-up (Nestlé), Nutilis (Nutricia Nordic AB), and Fresubin Clear (Fresenius Kabi GmbH), were injected into the model pharynx (15-ml volume). The preparation method used is described in **Paper II**. The resulting velocity profiles (Fig. 35) showed moderate shear-thinning behaviours, similar to those recorded in a continuous flow. In general, a broader velocity distribution was observed for all the thickened boluses, as compared to, for example, a fluid in continuous flow. This is due to the incorporation of air during mixing at the bolus formation and pumping stages. Thickener powders are generally composed of several ingredients apart from the main thickening agent, i.e., gum or starch. Of these ingredients, starch in its modified form has surface-active properties that result in air bubbles becoming entrapped in the bolus (Murray *et al.*, 2011).

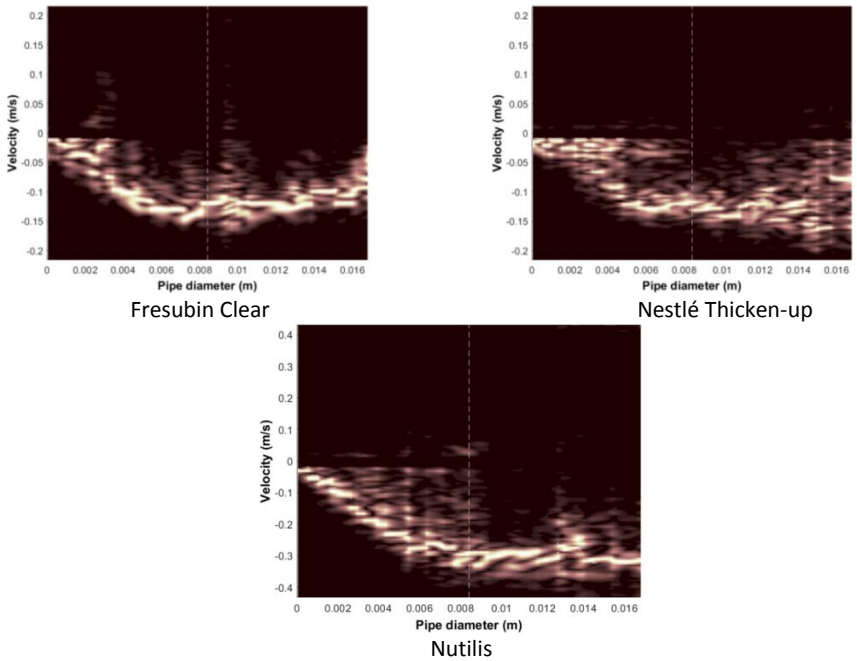

Figure 35: Velocity profiles of the boluses made with different commercial thickeners.

An appropriate bolus volume is required to be exposed to the transmitted ultrasound pulses, ensuring that the cavity is filled (no vacuum) while the ultrasound pulses hit the fluid in motion. The ultrasound sensor is vigilantly placed on the dorsal side of the model pharynx, so that there is maximum contact with the bolus during the flow and also that it resembles the bolus flow in human swallowing. The velocity profiles of the Thicken-up and Nutilis samples are distorted and incomplete on the far wall (right-hand side of the dividing line in the image; Fig. 35) due to multiple scattering. This is not a concern in the UVP technique, as half of the velocity profile, from the wall to the centre of the pipe is needed for the rheological calculation.

8.2 Materials and methods for velocity profiling and the resulting shear rate, following the NDD guidelines for bolus consistency

To perform further bolus analyses, the Nutilis thickener powder was used in the experiments in the rest of the bolus analysis (in **Paper IV**), due to its easy availability and versatility. As Nutilis contains both gum and starch as ingredients, it expresses a broad range of fluid properties, such as amylase resistance and easy solubility. The given powdered thickener was dissolved in water in the amounts listed in Table 4, while the mixing process used was the same as that described in **Paper II**.
The powdered thickener Nutilis was used in the experiment. Five different bolus consistencies were mixed (Table 4) with the given thickener. The thickener was added to water such that the consistency was in the range of 0.14–2.0 Pa.s at a shear rate of 50 s^{-1}, thereby covering the consistency range (NDD scale) from Nectar-thick (51–350 mPa.s) to pudding-thick (>1750 mPa.s). As the three viscosities used in the experiments lie in the honey-thick range (351–1750 mPa.s), this range of consistencies is further categorised into low, medium, and high consistencies to simplify the interpretation in the Discussion.

Table 4: Amount of thickener powder added to 100 ml water to achieve the different viscosities.

Viscosity at 50 s^{-1} (Pa.s)	Added powder (g)	NDD description
0.14±0	4.2	Nectar-thick
0.5±0.01	4.9	Low honey-thick
1.0±0.0	5.8	Medium honey-thick
1.5± 0.076	7.15	High honey-thick
2.0±0.09	7.8	Pudding-thick

8.3 Bolus velocity profiles and resulting shear rate measurements during model swallowing

The measured velocity profiles of the boluses thickened to consistencies of 0.2, 0.5, 1.0, 1.5 and 2.0 Pa.s (at 50 s^{-1}) are reported in Figure 36 (A–E) as power spectra, in which the brightness level is proportional to the power of the Doppler signal component at a given depth. The range of consistencies was selected following the NDD scale and covering all the consistencies from nectar-thick to pudding-thick, with the exception of the thin-liquid consistency, which was too thin for the current *in vitro* model to handle. The bolus of thin-liquid consistency often experienced a flow due to gravity, so it was not considered for further analysis. The velocity profiles presented in Figure 36 (A–E) were measured from the transducer side to the centre of the model pharynx, while the bolus flow was measured downwards away from the transducer depicted in negative values for the velocities.

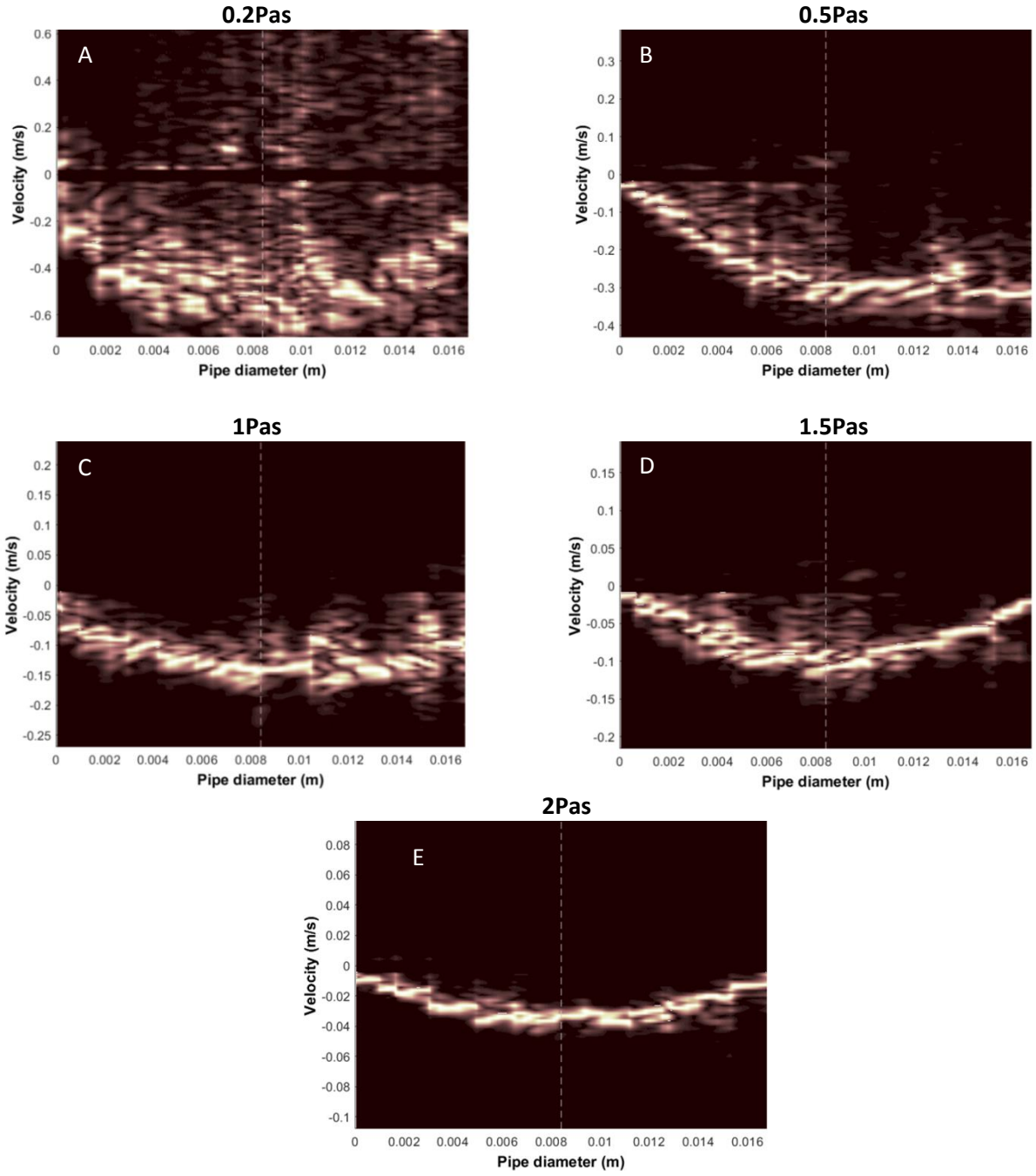

Figure 36: Velocity profiles acquired with ultrasound velocimetry using the Nutilis thickener to generate five different viscosities at 50 s^{-1}*: 0.2, 0.5, 1.0, 1.5, and 2.0 Pa.s*

During the measurements performed at constant velocity of the syringe (1.25±0.03 m/s), the average fluid velocities ranged from 0.046±0.02 m/s to 0.48±0.05 m/s, increasing in the order of increasing bolus consistency (Table 5). In general, the increased velocity that resulted from a low viscosity yielded higher shear rates, as expected. The variation in shear rate along the radial direction was calculated from the gradient of the acquired velocity profile (R^2~0.99). The calculated maximum shear rate (229±45 s^{-1}), as determined from the gradient of the recorded velocities at the wall, was highest for the nectar-thick formulation, which was the bolus with the lowest consistency (0.14 Pa.s). The bolus with pudding consistency (viscosity of 2.0 Pa.s at 50 s^{-1}), which was the highest consistency level used in the current work, yielded the lowest shear rate of 13±6 s^{-1}. This was followed by the high

honey-thick consistency (1.5 Pa.s at 50 s^{-1}), yielding a wall shear rate of 24±4 s^{-1}, while the boluses with medium and low honey-thick consistencies gave wall shear rates of 74±20 s^{-1} and 209±46 s^{-1}, respectively.

It is noteworthy that the level of brightness, which is an indicator of the quality of the measurement, was very high in the pudding-consistency sample (2.0 Pa.s at 50 s^{-1}). The quality of the signal deteriorated proportionally as the bolus consistency decreased, as seen for the bolus with nectar consistency, which had the lowest viscosity level used in the current work. There could be several reasons for this, such as a lower number of reflecting particles in low-viscosity fluids, excessive air accumulation while pumping the bolus, and the use of a lower number of pulses (128) to capture the average velocity profiles. Bolus transport is a rapid process, taking place in less than 1 second in healthy subjects and in the *in vitro* model used here. Therefore, much faster data acquisition is needed than, for example, what is required for a continuous fluid flow, as presented earlier (Section 7.3, laminar flow profiles), whereby the average profiles were based on 65,536 pulses. Furthermore, with increasing fluid velocities, the spectrum broadens due to presence of a wider range of velocities. Slight aliasing was noticed for the least-viscous fluid (Fig. 37 A) due to a mismatch between the PRF and observed fluid velocities.

The acquired bolus head velocities (0.48±0.05 m/s) observed here (Table 5) are comparable to those recorded in clinical studies. Tashiro and colleagues (Tashiro *et al.*, 2010) noted that the bolus velocity during pharyngeal flow varied from 0.246 m/s to 0.488 m/s. Hasegawa and co-workers (Hasegawa *et al.*, 2008) recorded an average velocity of 0.46 m/s for water, which decreased to 0.2 m/s upon the addition of thickeners to the water. Both studies used the Pulsed Ultrasound Doppler technique, the same method as used in the current sudy.

Typical values from most studies of velocity in the pharynx lie in the range of 0.1–0.5 m/s (Zhu *et al.*, 2014). In the present work, the ultrasound beam was directed towards the bolus flow above the epiglottis, i.e., in the meso-pharynx region. Knowledge regarding the velocity profile and subsequent shear rate in the meso-pharynx region is of clinical relevance owing to the higher risk of bolus misdirection in individuals who have a malfunctioning mechanism for air-ways closure.

Table 5: Shear viscosities, maximum velocities acquired, and the corresponding shear rates of boluses thickened to different consistencies according to the NDD scale.

Shear viscosity (Pa.s) at 50 s^{-1}	Maximum velocity (m/s)	Wall shear rate (1/s)	Description as per NDD
0.14	0.48±0.05	229±45	Nectar-thick
0.50	0.39±0.14	209.00±46	Low honey-thick
1.00	0.21±0.09	74.00±20	Medium honey-thick
1.50	0.09±0.020	22.00±5	High honey-thick
2.00	0.04±0.00	13.00±6	Pudding-thick

To our knowledge, only two studies have reported the bolus shear rate during pharyngeal swallowing: the study of Zhu *et al.* (Zhu *et al.*, 2014); and a simulation-based analysis conducted by Salinas and co-workers (Salinas-Vázquez *et al.*, 2014). Zhu *et al.* performed their study using video flouoscopy

on three human volunteers. The average shear rate reported was120 s^{-1}. Salinas *et al*. reported a higher shear rate (200 s^{-1}) along the pharyngeal wall. These values are in the vicinity of the current study.

Our results regarding shear rate during swallowing suggest that while the shear rate of 50 s^{-1} recommended by NDD is a reasonable value for fluids that are thickened to medium honey-thick consistency, the shear rate value, 50s^{-1} should carefully be used in boluses of lower consistencies such as in the case of nectar-thick and thin consistencies on the NDD scale.

For example, assuming a shear rate of 50 s^{-1} for every consistency of a fluid, a patient who swallows thinner fluids, i.e., in the range of low honey-thick or nectar-thick, will encounter much higher velocities (and therefore, higher shear rates) than those recommended by NDD, and this might result in aspiration.

For future interventions for patients with swallowing disorders, we propose that for each recommended bolus consistency, the expected shear rates reported here should be considered, so as to avoid over-estimation or under-estimation of the apparent consistency during swallowing.

8.4 Injection pump control and optical bolus visualization using fast camera

The swallowing mechanism in humans adjusts itself to the bolus consistency, i.e., the tongue can generate a certain level of force to push the bolus through the pharynx, thereby acting as a stress control device (Mackley *et al.*, 2013). Ideally, a pressure sensor at the syringe in the model was desirable to measure and control the pressure applied on the bolus. Unfortunately, on the model syringe, there is no pressure sensor that measures the applied pressure. Therefore, the rate-controlled approach, whereby the speed with which the piston moves to push the bolus and which is regulatable from the installed compressed air regulator, was applied.

8.4.1 Injection pump control

A camera (Sony, DSC-RX100M5, Tokyo, Japan) installed at a distance of 10 cm from the flow injection pump was used to record the syringe speed, which was maintained at 1.5±0.03 m/s irrespective of the bolus volume and viscosity. During the acquisition of the sequential photographic images of the bolus flow (Fig. 37), the camera was operated in a high frame rate mode, capturing images at 500 frames per second, while the bolus was dyed blue or orange for enhanced visualisation. The acquired slow-motion videos were analysed using the Media Player, MPC-HC ver. 1.7.13 software in the high-precision mode to determine transit times. This is discussed very briefly below in the context of bolus flow and consistency.

8.4.2 Optical bolus visualisation

The model pharynx is transparent, which allow direct visualisation of the bolus transport. Therefore, bolus velocity was visualised with the camera mentioned earlier by a sequence of photographic images of the bolus flow. As shown in Figure 38, the model pharynx was empty at t=0 ms. The bolus progressively entered the pharynx, passed through, and exited at the UES. The bolus with viscosity of 1.0 Pa.s (at 50 s^{-1}) presented a shorter transit time of 374 ms upon exit (Fig. 37; upper panel). In contrast, the bolus with pudding consistency (Fig. 37; lower panel) having a viscosity of 2.0 Pa.s (50 s^{-1}) exhibited slower movement, resulting in a delayed pharyngeal exit and a transit time of ~ 1 second.

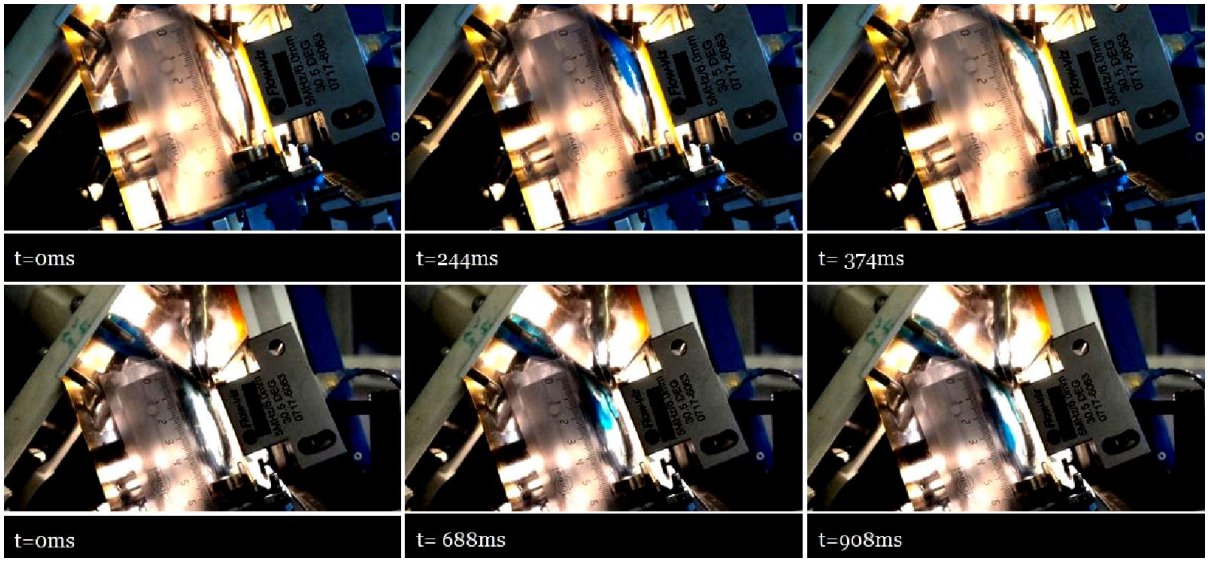

Figure 37: Photographic sequence of bolus ejection over time for boluses with viscosities of 1 Pa.s (upper panel) and 2 Pa.s (lower panel), at a shear rate of 50 s^{-1}.

As we have knowledge of the model pharynx geometry, as well as the average and maximum velocities calculated in UVP, the resulting transit times are approximately ~0.25 seconds and ~1 second, respectively, for the two displayed consistencies of 1.0 Pa.s and 2.0 Pa.s. Pharyngeal transit times that are typically reported from clinical studies range from 100 ms (Olthoff *et al.*, 2014) to 1 second as the bolus consistency increases. Therefore, the transit times reported here are in the range observed in clinical examinations.

8.5 *In vitro* manometry analysis

The pharyngeal swallow, which is a pressure-driven event that is initiated by the thrust of the tongue, requires complex co-ordination of different muscles to ensure safe bolus transport. Manometry is an important tool for examining abnormal swallowing processes in clinical studies. It is influenced by factors such as bolus consistency, volume, stenosis, and applied lingual pressure, among others. In the current *in vitro* model, the intra-bolus pressure, which is the pressure recorded as the fluid (bolus) comes in contact with the transducer, is measured. During clinical studies, there is often confusion in relation to distinguishing the contact pressure (the pressure recorded as the pressure transducer hits the pharyngeal wall) from the intra-bolus pressure. Inexperienced operators of manometry may easily confuse these two acquired values. In the following sections, bolus properties such as composition, consistency, and bolus volume are studied with respect to the pharyngeal pressures at different locations inside the *in vitro* model.

8.5.1 Manometry recorded using different thickeners during *in vitro* bolus flow

Table 6 presents a comparison of the pressures recorded by the transducers installed at the following locations in the model pharynx: pharynx entrance, mid-pharynx, and the UES. Of the three thickeners measured, Fresubin clear and Nutilis contain xanthan gum, while Nestlé Thicken-up contains starch as the thickener. The viscosities of the given fluids were set to 0.55 Pa.s (honey-thick consistency) at a shear rate of 50 s^{-1}. In general, the pressure applied in the model pharynx was significantly different ($p<0.05$) for boluses made from the three different thickeners, even though the viscosities were set to be similar at a shear rate of 50 s^{-1}. This was due to the compositions of the thickened fluids examined. Significantly ($p<0.05$) higher pressures were applied by the xanthan gum-based thickeners. In this category, Fresubin Clear recorded higher pressures (33.43±5.19–32.93±5.91 kPa) during model

swallowing than did Nutilis (21.43±0.06–17.75±2.56 kPa). The starch-based thickener, Nestlé Thicken-up, recorded significantly lower ($p<0.05$) pressures compared to the two gum-based thickeners used here. The reason for this is that a starch-thickened bolus stays together as a single mass and therefore applies a higher pressure (P=F/A) during swallowing than a bolus that is fragmented into many small parts.

Table 6: Manometry analysis of thickeners

Transducer location in the model pharynx	Fresubin clear (xanthan gum-based)	Nutilis (xanthan gum-based)	Nestlé Thicken-up (starch-based)
Pharyngeal entrance	$33.43^{a}\pm5.19^{1}$	$21.43^{b}\pm0.06^{1}$	$13.15^{c}\pm6.8^{1}$
Mid-pharynx	$32.64^{a}\pm5.76^{1}$	$19.47^{b}\pm0.16^{1}$	$6.12^{c}\pm4.38^{2}$
Close to the UES	$32.93^{a}\pm5.91^{1}$	$17.75^{b}\pm2.56^{1}$	$7.60^{c}\pm2.98^{23}$

Note: The different letters in the rows represent a statistically significant difference ($p<0.05$) among different thickeners, while the different numbers in the columns (after the standard deviation) represent a statistically significant difference ($p<0.05$) at different locations in model pharynx.

Furthermore, the pressure differences recorded at different locations in the model pharynx were noted to be smaller, and insignificantly different ($p<0.05$) for Fresubin Clear and Nutilis. This was not the case for the starch-thickened sample (with Nestlé Thicken-up), where a significant difference ($p<0.05$) was seen between the different locations, i.e., between the pharyngeal entrance and mid-pharynx and between the pharyngeal entrance and exit (Close the UES). Furthermore, during optical visualisation it was noticed that the starch-thickened bolus fell apart (due to having less elasticity) during the flow, resulting in smaller individual volumes and the appearance of residues on the pharyngeal walls (Fig. 38). As a consequence, significantly ($p<0.05$) lower pressure values were recorded for this category of thickener composition compared to the other gum-thickened compositions.

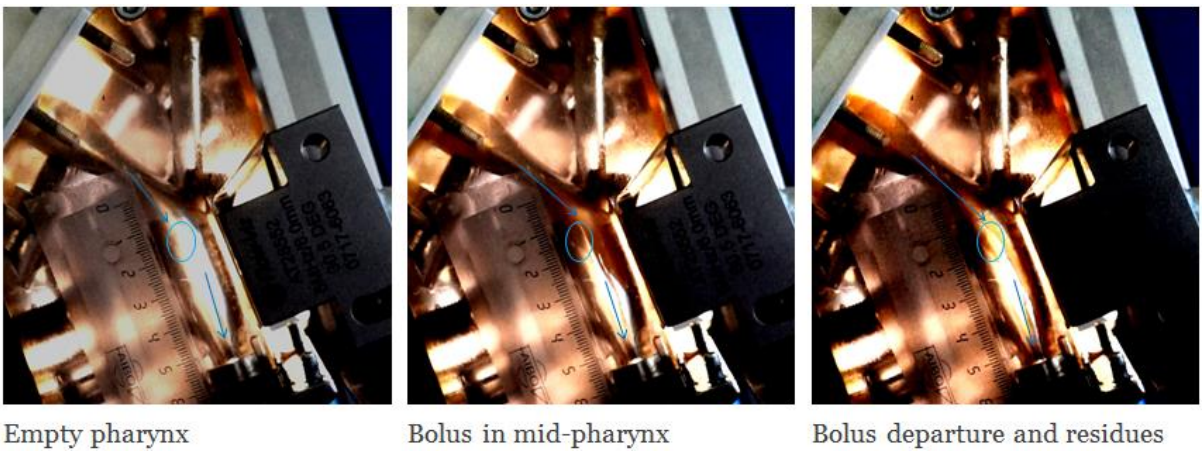

Figure 38: Photographic images showing (from left to right): the empty pharynx; a bolus inside the mid-pharynx; and bolus residues on the back and front walls at the exit of the model pharynx (coloured orange). The blue circles indicate the locations of residues of the disintegrated bolus (middle and right-most images). These residues are not visible in the blue circles in the left-most image, as the bolus had not yet been injected. The arrows in image shows normal bolus path

Clinical studies (Vilardell *et al.*, 2016) have shown that the use of starch-thickened boluses often leads to residues, and that the amounts of residues increase as the bolus consistency is increase to spoon-thick consistency (Newman *et al.*, 2016). Another study has reported that bolus residues increase when starch-thickened boluses with increasing volume are applied (Hadde, 2017), as was also noticed here (data not reported). The residue phenomenon detected with starch-thickened boluses *in vivo* is confirmed here during visualisation of the bolus path (Fig. 38). This was confirmed by the discovery of a lower pressure being exerted at the pharyngeal exit due to the bolus splitting into smaller volumes, as reported in Table 6.
A search of the literature for relevant *in vitro* studies revealed only one *in vitro* study (Redfearn *et al.*, 2018), which reported the pressure that resulted from applying a starch-thickened bolus was increased more than that for a gum-thickened bolus, as the area between the tongue and palate decreased. The mentioned literature study focused on manometry during the oral phase of swallowing of swallowing and therefore is not directly comparable to the current study.

8.5.2 Effect of bolus consistency using starch thickened boluses

Boluses that were thickened with a starch-based thickener (Nestlé Thicken-up) were further characterised by preparing formulations with different consistencies, ranging from Thin-liquid to Pudding-thick, according to the NDD scale. This was achieved by adding to water the powdered thickener at different concentrations (following the manufacturer's guidelines). This was done to study the influence of bolus consistency on the *in vitro* manometry during swallowing, while the starch-thickened boluses were used to explore further the observations described in the previous section (appearance of residues with starch-thickened fluids).
Our results show that bolus consistency increases the pharyngeal pressure (Fig. 39). The values were higher at the pharyngeal entrance, with the exception of the bolus with thin-liquid consistency (1–50 mPa.s) for which higher pressures were recorded at the mid-pharynx (2.31 kPa) and the UES (1.56 kPa), as compared to the pressure values at the pharyngeal entrance (1.26 kPa). This is due to free flow (gravity induced) of the thin consistency bolus. For this reason, boluses of thin consistency were not analysed further in the model, as the model is not capable of handling lower-level consistencies (similar to that of water).

Significantly ($p<0.05$) lower pressure values were recorded in the mid-pharynx for bolus consistencies in the higher range (honey and pudding), as compared to the pressure at the pharyngeal entrance. These differences were not statistically significant ($p<0.05$) at the mid-pharynx and the UES.
These findings further strengthen our argument that a starch-thickened bolus disintegrates during pharyngeal transport, resulting in residues being formed in the pharynx. As a consequence, there appears a smaller-volume bolus fraction, which applies lower pressures in the mid-pharynx and at the UES. This behavior of starch-thickened boluses needs to be confirmed in clinical studies. To the best of our knowledge, not a single study with similar focus has been published to date.

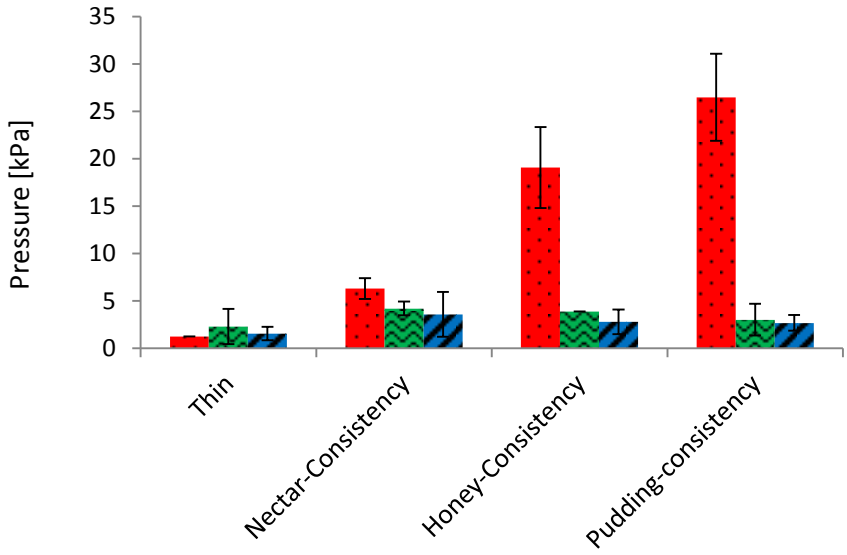

Figure 39: Influence of bolus consistency on the pressures recorded at different locations in the model pharynx during the pumping of starch-thickened boluses (Nestlé Thicken-up).

Bolus consistency is an important variable to consider in dysphagia management. The use of an appropriate bolus consistency improves the safety of swallowing in individuals who are suffering from malfunctioning deglutition (Yue *et al.*, 2017). While the results of clinical studies are more directly relevant to these patients they do not provide consistent conclusions. For example, Butler and co-workers (Butler *et al.*, 2009) reported no significant association between bolus consistency and pressure applied in the pharynx, whereas Yue *et al*. (Yue *et al.*, 2017) reported that the bolus pressure increased with decreasing bolus consistency. Ryu and colleagues (Ryu *et al.*, 2016) found the highest pressures, in the range of 210–232 mmHg (~28–31 kPa) for bread and thin-fluids, respectively, indicating no significant ($p<0.05$) differences between the consistencies of a 5-ml bolus. Similarly, research conducted by Lin and co-workers (Lin *et al.*, 2014) on boluses of different consistencies, i.e., water, and thick and paste-like boluses gave pressure values of 191, 173 and 181 mmHg (~25, 23, and 24 kPa), respectively. These differences in pressure are not significant ($p<0.05$) with respect to the different bolus consistencies

8.5.3 Effect of bolus volume

Since bolus volume is a vital factor in abnormal deglutition examinations, it has been considered in several *in vivo* research studies (W. Dodds *et al.*, 1988; Hoffman *et al.*, 2010; Lin *et al.*, 2014; Nascimento *et al.*, 2015). In clinical studies, a bolus volume of up to 20 ml has been reported (Hoffman *et al.*, 2010). In the current study (**Paper IV**), when the bolus volume was varied in the range of5–25 ml (which corresponds to a normal bolus volume) it was observed that changing the bolus volume had an impact on the pressure recorded at different locations in the model pharynx (Fig. 40). The Nutilis powder was used as the thickener for studying the bolus volume, so as to maintain the viscosity in the honey-thick-consistency range, specifically at ~0.50 Pa.s at $50.s^{-1}$.

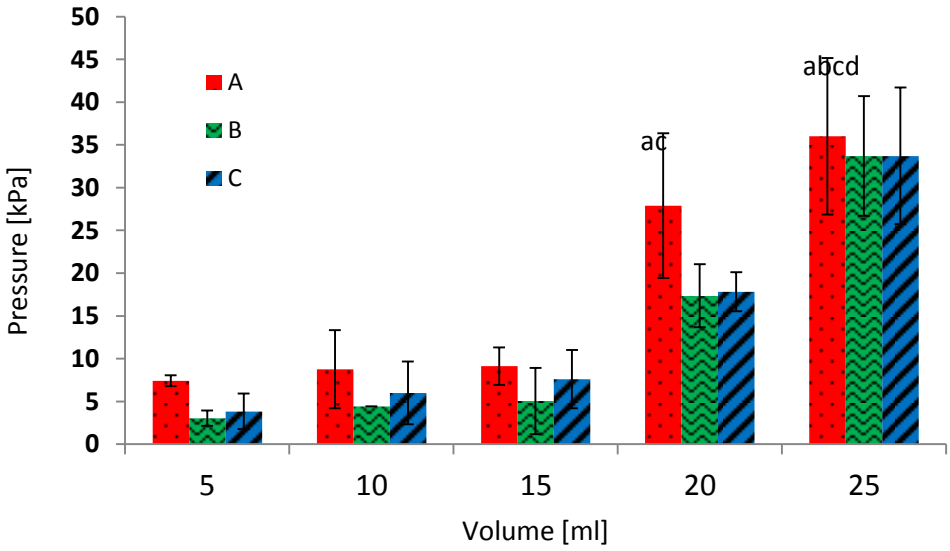

Figure 40. Means and standard deviations of the pressures recorded as a function of bolus volume (using Nutilis as the thickener) at different locations inside the model pharynx: A, pharynx entrance; B, mid-pharynx; and C, and close to the UES. Significantly different results with respect to the volume at Transducer A are lettered as follows: [a]p<0.05 vs 5-ml bolus; [b]p<0.05 vs 10-ml bolus; [c]p<0.05 vs 15-ml bolus; and [d]p<0.05 vs 20-ml bolus.

The volumes of bolus injected into the model pharynx could be categorised into two sets; low bolus volumes of 5, 10, and 15 ml; and high bolus volumes of 20 and 25 ml. In the low-bolus-volume category, the pressure values increased slightly but not significantly ($p<0.05$; Transducer A) due to their being too little a difference in the individual bolus volumes. Within the high-bolus-volume category, the pressure values were significantly different ($p<0.05$; Transducer A) between the 20-ml and 25-ml volumes. When a comparison was made between the low and high categories of bolus volumes, a significant difference ($p<0.05$; Transducer A) was observed. A similar trend of high volume and high pressure was noticed at the mid-pharynx transducer and at the pharyngeal exit transducer.

The recorded pressures were lower at the mid-pharynx with bolus volumes of 5, 10, 15 and 20 ml, due to the location of the transducer. The mid-pharynx transducer is located behind the epiglottis, and the epiglottis was closed to prevent fluid flow into the model airways, thereby restricting air-flow and resulting in lower measured pressures. The pressure values at the UES were higher than those in the mid-pharynx and lower than those at the model pharynx entrance, with respect to different fluid volumes.

A clinical study conducted by Lin and co-workers (Lin *et al.*, 2014) found pressure values of 202 mmHg and 173 mmHg (~27 and 23 kPa) for boluses of volumes of 5 ml and 10 ml, respectively. This meant that lower pressure values were recorded with increasing bolus volume. Similarly, studies carried out by Butler (Butler *et al.*, 2009) and Ryu (Ryu *et al.*, 2016) did not notice any significant association between the bolus volume and the pressure applied during pharyngeal bolus transport. In both of these instances, bolus volumes of 5 ml and 10 ml were used. However, Hoffman and colleagues (Hoffman *et al.*, 2010) noticed an increase in pharyngeal pressure accompanied by prolonged UES opening and longer pharyngeal pressure duration, when the bolus volume was increased to 20 ml

Clearly, the use of a higher bolus volume is more practical, even though this is avoided in clinical studies due to the discomfort experienced by the subjects. In contrast, in the simulator, bolus volumes up to 25 ml can be pumped in multiple times.

The clinical studies that have been performed to date have examined various aspects of swallowing, such as examinations of the bolus consistencies and biomechanical events, i.e., UES opening/contraction, duration of UES relaxation, pharyngeal peristaltic waves, and the onset of hyoid bone elevation while swallowing boluses of different volumes. Obviously, these biomechanical events cannot be mimicked in the current *in vitro* model. Moreover, the manometry results acquired here are not directly comparable to the results obtained from clinical manometry. The pressure values recorded in most clinical studies are within the range of 10–40 kPa, which overlaps to a large extent with the range of pressure values (~3–36 kPa) recorded here.

9. CONCLUSIONS

The work described in this thesis encompasses the methodology used and results obtained for a device that was developed to facilitate non-invasive, *in vitro* examinations of deglutition. In addition, the work elucidates the linkages between food bolus rheology and dysphagia management.

Fluid elasticity, i.e., the ability of a fluid to resist elongation, was studied as a factor for safe swallowing in individuals with malfunctioning deglutition. Model Boger fluids (elastic fluids with fixed viscosity) and fluids with even higher elasticity that were shear-thinning were comparatively easy to swallow, as evidenced by quantitative video fluoroscopy and when the patients were asked for sensory feedback on the ease of swallowing.
Fluids that are used for dysphagia management were further characterised for rheological properties that might influence the safety of swallowing in patients, such as extensional viscosity and yield stress, as well as the relatively well-known attribute of shear viscosity. Gum-based thickeners were found to be more elastic and more shear-thinning with a mild yield stress, as compared to starch-based thickeners. The yield stress noted for the gum-based thickener is attributed to a stranded, weak network structure that is visible on the nanometre scale in electron microscopy.

To overcome some of the challenges related to developing new treatments for patients with dysphagia, including issues of ethics and patient discomfort, an *in vitro* swallowing device was designed based on the human geometry that generates a realistic bolus flow and takes into account parameters of clinical interest, such as bolus velocity, bolus viscosity, and bolus volume. The device, *the Gothenburg Throat*, is the first of its kind that allows the performance of non-invasive bolus velocimetry and manometry simultaneously. The device can simulate various physiological actions such as opening/closing of the airways and UES and post-swallowing air release. To perform measurements inside the model pharynx, a comprehensive ultrasound velocimetry method based on a non-invasive transducer system was developed. Similarly, pressure transducers with the ability to measure intra-bolus pressure in the range reported from clinical studies were installed at different locations, at the pharyngeal entrance mid-pharynx, nasopharynx, and pharyngeal exit. Initially, both the ultrasound method and pressure transducers were validated during the continuous flow of fluids with different rheological properties and pumped at different flow rates. Thereafter, measurements of the bolus flow properties were performed.

The ultrasound velocimetry preformed here provides information about bolus transport similar to that obtained in clinical examinations using video fluoroscopy. While performing velocimetry on boluses thickened to consistencies listed in the NDD scale, the shear rates during bolus flow were observe to range from 13 s^{-1} for the pudding-thick consistency to 230 s^{-1} for the nectar-thick consistency, representing a much wider range of shear rates than that currently recognized by the NDD i.e., 50 s^{-1}. The optical observations were complemented by experiments of *in vitro* deglutition to capture other relevant features, such as the appearance of bolus residues during transit. It was found that a starch-thickened bolus often disintegrate during flow, leaving residues on the walls of the model pharynx. In

contrast, the gum-thickened boluses stay together as a single mass and do not deposit residues during pharyngeal transport. Similarly, the pressure transducers perform the clinical equivalent of manometry measurements. The manometry results acquired here for different thickeners, bolus consistencies, and bolus volumes are similar to those obtained with *in vivo* manometry. Therefore, the simulator is a promising tool for use by industry when designing food products for patients who are suffering from dysphagia.

10. FUTURE OUTLOOK

The results of the current project can be extended and refined in many directions in the future, some of which are discussed below.

The *Gothenburg throat* model device can be further refined and improved to provide even more accurate measurements. An extra pressure transducer should be installed to measure the applied pressure on the bolus, thereby conferring better control over the data obtained for the applied pressure. The air-ways closing mechanism should be improved to achieve better simulation of abnormal deglutition. This would enable the study of elastic fluid flows during *in vitro* deglutition, while simulation studies could be performed in parallel to compare the results.

The simulator has a built-in nasal cavity to recover flavour compounds upon post-swallow air release Experiments were performed on flavour release in the model (which are not reported here as this topic is beyond the scope of this thesis) by capturing the released air and analysing it using gas chromatography. The results confirm the release of the flavour compound that was added to fluids thickened to different consistencies and that had different compositions. Further studies should be performed to build knowledge as to how the rheology of a matrix influences the flavour release afrer the swallowing thrust triggered by the tongue and at body temperature. This would open the possibility to tailor food products that are not only safe for swallowing but also have high palatability.

Similarly, when using ultra-sonics, the shear rate should be measured at other locations, such as in the hypopharynx and at the UES, as the areas and velocities vary significantly in these regions. The UVP software should be upgraded to perform fast data acquisition and to have an improved graphical display, especially during analyses of bolus transport. This would allow real-time observations of bolus transport. The current system is restricted to post-processing of the acquired data.

The pharyngeal phase is followed by the esophageal phase, which should be rather easy to simulate given that a flexible model esophageal tube is already connected to the model pharynx. Peristaltic movement of the bolus can be simulated in the model esophagus tube by connecting a series of motor-controlled rollers.

Acknowledgments

During the past, four and half years, many people contributed towards the completion of this project and I am grateful to each and every one of them.

Such as:

- My principle supervisor, Dr Mats Stading for introducing me to the very unique and exciting knowledge of rheology. His constructive feedback, constant support and guidance, useful scientific discussions and wonderful company while travelling together is highly commendable.
- I am equally thankful to Dr Olle Ekberg for introducing me to clinical examinations, and practical knowledge of human physiology and x-ray video fluoroscopy. Olle Ekberg was always available for each and every single query I had during the course of this project, even though he was at a distance which I really appreciate.
- I am grateful to my co-supervisor, Johan Wiklund for allowing me to work with very advance form of rheology, UVP+PD. I feel very lucky to have worked with such a fascinating technique. I am equally grateful to Reinhardt Kotze (Incipientous) for his help, guidance and instant availability on UVP measurements.
- My examiners Antal Boldizar and Mikael Rigdahl at Chalmers for their guidance and follow up of my progress and their useful advises.
- Most importantly I would like to acknowledge the colleagues at Product Design and Perception group that later became good friends. I felt so attached to the group and my work place due to the positive and supportive environment created by the whole group. And this list includes all the new employees, senior employees and diploma students and former PhD students during transitions from SIK to SP and now RISE. The merging of sensory and aroma section to our original structure group was an even more pleasant addition. I acknowledge my office-mates Emma Bragd and Tommy Dam for their nice company and encouragement during the course of this project. Besides PDP, the other sections at RISE; environment, process technology and Microbiology. Moreover, the administration at RISE are highly appreciated for their help and pleasantries during my stay at RISE.
- I also acknowledge Frederik Holmberg for the technical assistance in this project

- I would like to thank all the member of the evaluation committee for sparing their precious time to evaluate this work.
- The companies (Fresenius-Kabi, Nestle healthcare, Nutricia, Findus, and Dansukker Malmö, Sweden) which kindly provided their samples

- I acknowledge Golfclub restaurant's team for providing high quality food at RISE
- I am very grateful to all my friends who continuously support and motivated me to reach to this point, the list is huge and the most immediate ones are: Manish Prakash, Shahzeb Anwer, Rashid Mansoor, Shahid Khan, Afzal khan, Anver Hisham, Mustafa, Yessica and many more.
- Finally I would like to express my gratitude to my family: parents, brothers and sisters, uncles, aunts, cousins and grand-parents for their rock-solid support and their powerful prayers that led my way during this journey.

Waqas Qazi

REFERENCES

Adam S Burbidge, J. A. Y. C., Jan Engmann, Catirona M. Steele. (2016). A day in the life of the fluid bolus: An introduction to fluid mechanics of the oropharyngeal phase of swallowing with particular focus on dysphagia. *Appl. Rheology, 5*(26), 10.

Alsanei, W. A., & Chen, J. (2014). Studies of the Oral Capabilities in Relation to Bolus Manipulations and the Ease of Initiating Bolus Flow. *Journal of Texture Studies, 45*(1), 1-12. doi: 10.1111/jtxs.12041

Anne Laure Koliandris, E. R., Louise Hewson, Joanne Hort, Andrew Taylor, Bettina Wolf. (2010). *Food Grade Boger fluid for sensory studies.* (21). (1)

Barnes, H. A. (1995). A review of the slip (wall depletion) of polymer solutions, emulsions and particle suspensions in viscometers: its cause, character, and cure. *Journal of Non-Newtonian Fluid Mechanics, 56*(3), 221-251.

Barnes, H. A., Hutton, J. F., & Walters, K. (1997). *An Introduction to Rheology*: Elsevier.

Berta, M., Wiklund, J., Kotzé, R., & Stading, M. (2016). Correlation between in-line measurements of tomato ketchup shear viscosity and extensional viscosity. *Journal of Food Engineering, 173*, 8-14. doi: http://dx.doi.org/10.1016/j.jfoodeng.2015.10.028

Binding, D. M., & Jones, D. M. (1989). On the interpretation of data from Converging Flow Rheometers. *Rheologica Acta, 28*(3), 215-222. doi: 10.1007/BF01332853

Bohlin, W. a. (1999). Extensional Flow Studies of Wheat Flour Dough. I. Experimental Method for Measurements in Contraction Flow Geometry and Application to Flours Varying in Breadmaking Performance. *Journal of Cereal Science, 29*(3), 217-226. doi: http://dx.doi.org/10.1006/jcrs.1999.0251

Butler, S. G., Stuart, A., Castell, D., Russell, G. B., Koch, K., & Kemp, S. (2009). Effects of Age, Gender, Bolus Condition, Viscosity, and Volume on Pharyngeal and Upper Esophageal Sphincter Pressure and Temporal Measurements During Swallowing. *Journal of Speech, Language, and Hearing Research, 52*(1), 240-253.

Bülow, M. (2003). Therapeutic aspects of oral and pharyngeal swallowing dysfunction.

Cassiani, R. A., Santos, C. M., Parreira, L. C., & Dantas, R. O. (2011). The relationship between the oral and pharyngeal phases of swallowing. *Clinics, 66*(8), 1385-1388. doi: 10.1590/S1807-59322011000800013

Chen, F. J., Dirven, S., Xu, W. L., Bronlund, J., Li, X. N., & Pullan, A. (2012). Review of the swallowing system and process for a biologically mimicking swallowing robot. *Mechatronics, 22*(5), 556-567. doi: 10.1016/j.mechatronics.2012.02.005

Chen, J., & Lolivret, L. (2011). The determining role of bolus rheology in triggering a swallowing. *Food Hydrocolloids, 25*(3), 325-332. doi: https://doi.org/10.1016/j.foodhyd.2010.06.010

Clavé, P., De Kraa, M., Arreola, V., Girvent, M., Farre, R., Palomera, E., & SERRA-PRAT, M. (2006). The effect of bolus viscosity on swallowing function in neurogenic dysphagia. *Alimentary pharmacology & therapeutics, 24*(9), 1385-1394.

Dodds, W., Man, K., Cook, I., Kahrilas, P., Stewart, E., & Kern, M. (1988). Influence of bolus volume on swallow-induced hyoid movement in normal subjects. *American Journal of Roentgenology, 150*(6), 1307-1309.

Dodds, W. J. (1989). The physiology of swallowing. *Dysphagia, 3*(4), 171-178. doi: 10.1007/bf02407219

Ekberg, O., Hamdy, S., Woisard, V., Wuttge–Hannig, A., & Ortega, P. (2002). Social and psychological burden of dysphagia: its impact on diagnosis and treatment. *Dysphagia, 17*(2), 139-146.

Ekberg, O., Stading, M., Johansson, D., Bülow, M., Ekman, S., & Wendin, K. (2010). Flow properties of oral contrast medium formulations depend on the temperature. *Acta Radiologica, 51*(4), 363-367. doi: 10.3109/02841851003645751

Ferguson, J., Walters, K., & Wolff, C. (1990). Shear and extensional flow of polyacrylamide solutions. *Rheologica Acta, 29*(6), 571-579.

Gallegos, C., Brito-de la Fuente, E., Clavé, P., Costa, A., & Assegehegn, G. (2016). Nutritional Aspects of Dysphagia Management. *Advances in Food and Nutrition Research*.

Hadde. (2017). Understanding the Rheological Parameters of Thickened Fluids for Dysphagia Sufferers *PhD thesis (University of Queensland)*.

Hasegawa, A., Nakazawa, F., & Kumagai, H. (2008). Velocity of Swallowed Food for Dysphagic Patients Through the Pharynx by Ultrasonic Method. *Nippon Shokuhin Kagaku Kogaku Kaishi, 55*(11), 541-548. doi: 10.3136/nskkk.55.541

Hoffman, M. R., Ciucci, M. R., Mielens, J. D., Jiang, J. J., & McCulloch, T. M. (2010). Pharyngeal swallow adaptations to bolus volume measured with high resolution manometry. *The Laryngoscope, 120*(12), 2367-2373. doi: 10.1002/lary.21150

James, D. F. (1991). Flow in a converging channel at moderate reynolds numbers. *AIChE Journal, 37*(1), 59-64. doi: 10.1002/aic.690370105

Jensen, J. A. (1996). *Estimation of Blood Velocities Using Ultrasound: A Signal Processing Approach*: Cambridge University Press.

John, L. (2007). Viscous flow through pipes of various cross-sections. *European Journal of Physics, 28*(3), 521.

Joshi, M. M., Joshi, S. S., & Joshi, S. D. (2011). The morphological study of adult human larynx in a Western Indian population. *Journal of Laryngology and Voice, 1*(2), 50.

Kano, M., Shimizu, Y., Okayama, K., Igari, T., & Kikuchi, M. (2005). A morphometric study of age-related changes in adult human epiglottis using quantitative digital analysis of cartilage calcification. *Cells Tissues Organs, 180*(2), 126-137.

Kocsis, K. (1995). Techniques in rheological measurements. *6*. doi: 10.1016/0956-7143(9590023-3)

Leonard, R. J., White, C., McKenzie, S., & Belafsky, P. C. (2014). Effects of Bolus Rheology on Aspiration in Patients with Dysphagia. *Journal of the Academy of Nutrition and Dietetics, 114*(4), 590-594. doi: http://dx.doi.org/10.1016/j.jand.2013.07.037

Lin, T., Xu, G., Dou, Z., Lan, Y., Yu, F., & Jiang, L. (2014). Effect of bolus volume on pharyngeal swallowing assessed by high-resolution manometry. *Physiology & Behavior, 128*, 46-51. doi: https://doi.org/10.1016/j.physbeh.2014.01.030

Mackley, M. R., Tock, C., Anthony, R., Butler, S. A., Chapman, G., & Vadillo, D. C. (2013). The rheology and processing behavior of starch and gum-based dysphagia thickeners. *Journal of Rheology (1978-present), 57*(6), 1533-1553. doi: doi:http://dx.doi.org/10.1122/1.4820494

Marcotte, M. (2001). Rheological properties of selected hydrocolloids as a function of concentration and temperature. *Food Research International, 34*(8), 695-703. doi: http://dx.doi.org/10.1016/S0963-9969(01)00091-6

Mashimo, G. a. (2006). Physiology of oral, pharyngeal, and esophageal motility. *GI Motility online*. doi: doi:10.1038/gimo1

McFarland, D. H., Martin-Harris, B., Fortin, A. J., Humphries, K., Hill, E., & Armeson, K. (2016). Respiratory-swallowing coordination in normal subjects: Lung volume at swallowing initiation. *Respiratory Physiology & Neurobiology, 234*, 89-96. doi: http://doi.org/10.1016/j.resp.2016.09.004

Moret-Tatay, Rodríguez-García, J., Martí-Bonmatí, E., Hernando, I., & Hernández, M. J. (2015). Commercial thickeners used by patients with dysphagia: Rheological and structural behaviour in different food matrices. *Food Hydrocolloids, 51*, 318-326. doi: 10.1016/j.foodhyd.2015.05.019

Morinière, S., Hammoudi, K., Marmouset, F., Bakhos, D., Beutter, P., & Patat, F. (2013). Ultrasound analysis of the upper esophageal sphincter during swallowing in the healthy subject. *European Annals of Otorhinolaryngology, Head and Neck Diseases, 130*(6), 321-325. doi: http://dx.doi.org/10.1016/j.anorl.2012.01.008

Mowlavi, S., Engmann, J., Burbidge, A., Lloyd, R., Hayoun, P., Le Reverend, B., & Ramaioli, M. (2016). In vivo observations and in vitro experiments on the oral phase of swallowing of Newtonian and shear-thinning liquids. *Journal of Biomechanics, 49*(16), 3788-3795. doi: http://doi.org/10.1016/j.jbiomech.2016.10.011

Murray, B. S., Durga, K., Yusoff, A., & Stoyanov, S. D. (2011). Stabilization of foams and emulsions by mixtures of surface active food-grade particles and proteins. *Food Hydrocolloids, 25*(4), 627-638. doi: https://doi.org/10.1016/j.foodhyd.2010.07.025

Nahar, S., Jeelani, S. A. K., & Windhab, E. J. (2012). Influence of elastic tube deformation on flow behavior of a shear thinning fluid. *Chemical Engineering Science, 75*(0), 445-455. doi: http://dx.doi.org/10.1016/j.ces.2012.03.051

Nascimento, W. V., Cassiani, R. A., Santos, C. M., & Dantas, R. O. (2015). Effect of Bolus Volume and Consistency on Swallowing Events Duration in Healthy Subjects. *Journal of Neurogastroenterology and Motility, 21*(1), 78-82. doi: 10.5056/jnm14055

Newman, R., Vilardell, N., Clavé, P., & Speyer, R. (2016). Effect of Bolus Viscosity on the Safety and Efficacy of Swallowing and the Kinematics of the Swallow Response in Patients with Oropharyngeal Dysphagia: White Paper by the European Society for Swallowing Disorders (ESSD). *Dysphagia, 31*(2), 232-249. doi: 10.1007/s00455-016-9696-8

Nishinari, K., Takemasa, M., Su, L., Michiwaki, Y., Mizunuma, H., & Ogoshi, H. (2011). Effect of shear thinning on aspiration – Toward making solutions for judging the risk of aspiration. *Food Hydrocolloids, 25*(7), 1737-1743. doi: 10.1016/j.foodhyd.2011.03.016

Nyström, M., Jahromi, H. T., Stading, M., & Webster, M. (2017). Hyperbolic contraction measuring systems for extensional flow. *Mechanics of Time-Dependent Materials*, 1-25.

Olthoff, A., Zhang, S., Schweizer, R., & Frahm, J. (2014). On the Physiology of Normal Swallowing as Revealed by Magnetic Resonance Imaging in Real Time. *Gastroenterology Research and Practice, 2014*, 10. doi: 10.1155/2014/493174

Petrie, C. J. S. (2006). Extensional viscosity: A critical discussion. *Journal of Non-Newtonian Fluid Mechanics, 137*(1–3), 15-23. doi: http://dx.doi.org/10.1016/j.jnnfm.2006.01.011

Popa Nita, S., Murith, M., Chisholm, H., & Engmann, J. (2013). Matching the Rheological Properties of Videofluoroscopic Contrast Agents and Thickened Liquid Prescriptions. *Dysphagia, 28*(2), 245-252. doi: 10.1007/s00455-012-9441-x

Redfearn, A., & Hanson, B. (2018). A Mechanical Simulator of Tongue–Palate Compression to Investigate the Oral Flow of Non-Newtonian Fluids. *IEEE/ASME Transactions on Mechatronics, 23*(2), 958-965. doi: 10.1109/TMECH.2018.2808704

Różańska, S. (2017). Chapter 6 - Extensional Rheology in Food Processing. In J. Ahmed, P. Ptaszek & S. Basu (Eds.), *Advances in Food Rheology and Its Applications* (pp. 125-157): Woodhead Publishing.
Ryu, J. S., Park, D., Oh, Y., Lee, S. T., & Kang, J. Y. (2016). The Effects of Bolus Volume and Texture on Pharyngeal Pressure Events Using High-resolution Manometry and Its Comparison with Videofluoroscopic Swallowing Study. *Journal of Neurogastroenterology and Motility, 22*(2), 231-239. doi: 10.5056/jnm15095
Salinas-Vázquez, M., Vicente, W., Brito-de la Fuente, E., Gallegos, C., Márquez, J., & Ascanio, G. (2014). Early Numerical Studies on the Peristaltic Flow through the Pharynx. *Journal of Texture Studies, 45*(2), 155-163. doi: 10.1111/jtxs.12060
Singh, R. P., & Heldman, D. R. (2009). *Introduction to Food Engineering*: Elsevier/Academic Press.
Singh, R. P., & Heldman, D. R. (2014). Chapter 1 - Introduction. In R. P. S. R. Heldman (Ed.), *Introduction to Food Engineering (Fifth Edition)* (pp. 1-64). San Diego: Academic Press.
Steele. (2015). The Blind Scientists and the Elephant of Swallowing: A Review of Instrumental Perspectives on Swallowing Physiology. *Journal of Texture Studies, 46*(3), 122-137. doi: 10.1111/jtxs.12101
Steele, Molfenter, S. M., Péladeau-Pigeon, M., Polacco, R. C., & Yee, C. (2014). Variations in Tongue-Palate Swallowing Pressures When Swallowing Xanthan Gum-Thickened Liquids. *Dysphagia, 29*(6), 678-684. doi: 10.1007/s00455-014-9561-6
Steele, C., Alsanei, W., Ayanikalath, S., Barbon, C. A., Chen, J., Cichero, J. Y., Coutts, K., Dantas, R., Duivestein, J., Giosa, L., Hanson, B., Lam, P., Lecko, C., Leigh, C., Nagy, A., Namasivayam, A., Nascimento, W., Odendaal, I., Smith, C., & Wang, H. (2015). The Influence of Food Texture and Liquid Consistency Modification on Swallowing Physiology and Function: A Systematic Review. *Dysphagia, 30*(1), 2-26. doi: 10.1007/s00455-014-9578-x
Steffe, J. F. (1996). *Rheological methods in food process engineering*: Freeman press.
Takeda, Y. (1995). Velocity profile measurement by ultrasonic doppler method. *Experimental Thermal and Fluid Science, 10*(4), 444-453. doi: http://dx.doi.org/10.1016/0894-1777(94)00124-Q
Tashiro, A., Hasegawa, A., Kohyama, K., Kumagai, H., & Kumagai, H. (2010). Relationship between the rheological properties of thickener solutions and their velocity through the pharynx as measured by the ultrasonic pulse Doppler method. *Bioscience, Biotechnology, and Biochemistry, 74*(8), 1598-1605.
Tobin, A. B., Heunemann, P., Wemmer, J., Stokes, J. R., Nicholson, T., Windhab, E. J., & Fischer, P. (2017). Cohesiveness and flowability of particulated solid and semi-solid food systems. *Food & Function, 8*(10), 3647-3653. doi: 10.1039/C7FO00715A
Walsh, J. H., Leigh, M. S., Paduch, A., Maddison, K. J., Philippe, D. L., Armstrong, J. J., Sampson, D. D., Hillman, D. R., & Eastwood, P. R. (2008). Evaluation of pharyngeal shape and size using anatomical optical coherence tomography in individuals with and without obstructive sleep apnoea. *Journal of Sleep Research, 17*(2), 230-238. doi: 10.1111/j.1365-2869.2008.00647.x
Wiklund, J., Shahram, I., & Stading, M. (2007). Methodology for in-line rheology by ultrasound Doppler velocity profiling and pressure difference techniques. *Chemical Engineering Science, 62*(16), 4277-4293. doi: 10.1016/j.ces.2007.05.007
Wiklund, J., & Stading, M. (2008). Application of in-line ultrasound Doppler-based UVP–PD rheometry method to concentrated model and industrial suspensions. *Flow Measurement and Instrumentation, 19*(3–4), 171-179. doi: http://dx.doi.org/10.1016/j.flowmeasinst.2007.11.002

Wikström, K., & and Bohlin, L. (1999). Extensional Flow Studies of Wheat Flour Dough. I. Experimental Method for Measurements in Contraction Flow Geometry and Application to Flours Varying in Breadmaking Performance. *Journal of Cereal Science, 29*(3), 217-226. doi: http://dx.doi.org/10.1006/jcrs.1999.0251
Wikström, K., & Bohlin, L. (1999). Extensional Flow Studies of Wheat Flour Dough. I. Experimental Method for Measurements in Contraction Flow Geometry and Application to Flours Varying in Breadmaking Performance. *Journal of Cereal Science, 29*(3), 217-226. doi: http://dx.doi.org/10.1006/jcrs.1999.0251
Vilardell, N., Rofes, L., Arreola, V., Speyer, R., & Clavé, P. (2016). A Comparative Study Between Modified Starch and Xanthan Gum Thickeners in Post-Stroke Oropharyngeal Dysphagia. *Dysphagia, 31*(2), 169-179. doi: 10.1007/s00455-015-9672-8

Yang, W., Fung, T. C., Chian, K. S., & Chong, C. K. (2007). Finite element simulation of food transport through the esophageal body. *World Journal of Gastroenterology : WJG, 13*(9), 1352-1359. doi: 10.3748/wjg.v13.i9.1352

Yue, L., Guang-qing, X., Fan, Y., Tuo, L., Li-sheng, J., & Feng, L. (2017). The effect of bolus consistency on swallowing function measured by high-resolution manometry in healthy volunteers. *The Laryngoscope, 127*(1), 173-178. doi: doi:10.1002/lary.26085

Zhu, J., Mizunuma, H., & Michiwaki, Y. (2014). Determination of Characteristic Shear Rate of a Liquid Bolus through the Pharynx during Swallowing. *Journal of Texture Studies, 45*(6), 430-439.